

(19)



(10) **FI 20106063 A7**

(12) **JULKISEksi TULLUT PATENTTIHAKEMUS  
PATENTANSÖKAN SOM BLIVIT OFFENTLIG  
PATENT APPLICATION MADE AVAILABLE TO THE  
PUBLIC**

(21) Patentihakemus - Patentansökan - Patent application **20106063**

(51) Kansainvälinen patenttiluokitus - Internationell patentklassifikation -  
International patent classification

**H03H 9/56 (2006.01)**

**H03H 3/02 (2006.01)**

(22) Tekemispäivä - Ingivningsdag - Filing date **14.10.2010**

(23) Saapumispäivä - Ankomstdag - Reception date **14.10.2010**

(41) Tullut julkiseksi - Blivit offentlig - Available to the public **08.06.2012**

(43) Julkaisupäivä - Publiceringsdag - Publication date **14.06.2019**

**SUOMI - FINLAND**

**(FI)**

**PATENTTI- JA REKISTERIHALLITUS  
PATENT- OCH REGISTERSTYRELSEN  
FINNISH PATENT AND REGISTRATION OFFICE**

(71) Hakija - Sökande - Applicant

**1 • Valtion teknillinen tutkimuskeskus**, Vuorimiehentie 3, 02150 ESPOO, SUOMI - FINLAND, (FI)

(72) Keksijä - Uppfinnare - Inventor

**1 • MELTAUS, Johanna**, VTT, SUOMI - FINLAND, (FI)  
**2 • PENSALA, Tuomas**, VTT, SUOMI - FINLAND, (FI)

(74) Asiamies - Ombud - Agent

**Seppo Laine Oy**, PL 339, 00181 Helsinki

(54) Keksinnön nimitys - Uppfinningens benämning - Title of the invention

**Akustisesti kytketty laajakaistainen ohutkalvo-BAW-suodatin**

**Akustiskt kopplat bredbandigt tunnfilms-BAW-filter**

**Wide-band acoustically coupled thin-film BAW filter**

(57) Tiivistelmä - Sammandrag - Abstract

Denna uppfinning avser ett akustiskt kopplat tunnfilms-BAW-filter, som omfattar ett piezoelektriskt skikt (1), en ingångsport (2) på det piezoelektriska skiktet (1) för att omvandla en elektrisk signal till en akustisk våg (SAW, BAW) och en utgångsport (3) på det piezoelektriska skiktet (1) för att omvandla en akustisk signal till en elektrisk signal. Enligt uppfinningen innehåller portarna (2, 3) elektroder (5, 6), som är anordnade i närheten av varandra, och filtret är designat att fungera i första ordningens tjockleksutsträckande TE1-mod.

Keksintö koskee akustisesti kytkettyä ohutkalvo-BAW-suodatinta, joka käsittää pietosähköisen kerroksen (1), tuloportin (2) pietosähköisellä kerroksella (1) sähköisen signaalin muuttamiseksi akustiseksi aalloksi (SAW, BAW) ja lähtöportin (3) pietosähköisellä kerroksella (1) akustisen signaalin muuttamiseksi sähköiseksi signaaliksi. Keksinnön mukaisesti portit (2, 3) sisältävät elektrodit (5, 6), jotka on sijoitettu lähelle toisiaan, ja suodatin on suunniteltu toimimaan ensimmäisen kertaluokan paksuusulottuvuussa TE1-muodossa.

## WIDE-BAND ACOUSTICALLY COUPLED THIN-FILM BAW FILTER

## FIELD OF INVENTION

5 The present invention relates to a wide-band acoustically coupled thin-film Bulk Acoustic Wave (BAW) filter according to the preamble of Claim 1.

## BACKGROUND OF THE INVENTION

Radio-frequency (RF) components, such as resonators and filters, based on microacoustics and thin-film technology are widely used in radio applications such as: mobile phones, 10 wireless networks, satellite positioning, etc. Their advantages over their lumped-element counterparts include small size and mass-production capability. Two fundamental microacoustic technologies used for RF devices are surface acoustic wave (SAW) and bulk acoustic wave (BAW) technologies.

15 In this section, existing filter technologies are briefly introduced to provide background for the current invention.

**Surface acoustic wave devices**

20 A schematic picture of a SAW device is shown in Fig. 1(a). Interdigital transducers (IDTs) 2, 3 (comb-like structures of thin-film metal strips) are patterned on a piezoelectric substrate 1. The piezoelectric substrate is, for example, quartz, LiNbO<sub>3</sub> or LiTaO<sub>3</sub>. The IDTs are used to transform the electric input signal  $V_{in}$  into an acoustic wave via the piezoelectric effect, as well as to pick up the acoustic signal at the output port and 25 transform it back to an electrical form. The operation frequency of a SAW device depends on the velocity of the acoustic wave and the dimensions of the IDT electrodes:

$$f \propto \frac{2p}{v}$$

where  $f$  is the frequency,  $p$  is the period of the IDT, see Fig. 1(b), and  $v$  is the velocity of the surface wave. Therefore, higher operation frequencies require smaller  $p$  if the velocity is kept constant.

5 SAW transducers are typically periodic, although the period may be more complex than that presented in Fig. 1.

### Bulk acoustic wave devices

10 In a BAW device, acoustic vibration inside a piezoelectric wafer or a thin film is used to process the electrical input signal. The piezoelectric material used for the thin film in the devices typically belongs to the 6mm symmetry group, e.g. ZnO, AlN and CdS. Other piezoelectric materials can be used as well, such as quartz, LiNbO<sub>3</sub>, LiTaO<sub>3</sub>, etc. A schematic cross-section of a solidly-mounted BAW resonator (SMR) is presented in Fig. 15 2(a) and of a self-supported (membrane type) resonator in Fig. 2(b). In an SMR, an acoustic Bragg mirror composed of alternating high and low acoustic impedance ( $Z$ ) material layers serves to isolate the vibration in the piezoelectric thin film from the substrate and to prevent acoustic leakage. In the membrane device the same is accomplished by fabricating the resonator on a self-standing membrane.

20

The area of a BAW resonator is typically determined by the static capacitance needed to match the device to the system impedance. Filters can be constructed of resonators by connecting resonators electrically. A common example is a ladder filter, in which resonators are connected in T- or Pi-sections (Fig. 3). Designing the resonance frequencies 25 appropriately, one can achieve a passband response. Increasing the number of sections helps to widen the passband. The out-of-band signal suppression is determined by the capacitances of the resonator structure and is typically on the order of ~25 dB. The in-band losses are mainly determined by the Q-values of the resonators.

30 **Vibration modes and dispersion types**

In the piezoelectric layer of an acoustic resonator, different bulk acoustic vibration modes arise as the excitation frequency  $f$  is swept. In BAW devices, the propagation direction of

the bulk wave is typically along the thickness axis (z axis). Particle displacement is either perpendicular to the propagation direction (shear wave) or parallel to the propagation direction (longitudinal wave). Bulk modes are characterized by the number of half-wavelengths of the bulk wavelength  $\lambda_z$  that can fit into the thickness of the resonator 5 structure (piezoelectric layer and electrodes). In addition, the bulk modes can propagate in the lateral (perpendicular to z-axis) direction as plate waves with lateral wavelength  $\lambda_{\parallel}$ . This is illustrated in Fig. 4a for two bulk modes (longitudinal and shear). In a finite-sized resonator, plate waves reflecting from resonator edges can cause laterally standing waves and consequently lateral resonance modes.

10

Acoustic properties of a BAW resonator can be described with dispersion curves, in which the lateral wave number  $k_{\parallel}$  of the vibration is presented as a function of frequency. Fig. 4b shows an example of dispersion properties in a BAW resonator. Dispersion curves of the electroded (active) region are plotted with a solid line and those of the non-electroded 15 (outside) region with dashed line. The first-order longitudinal (thickness extensional, TE1) vibration mode, in which the thickness of the piezoelectric layer contains approximately half a wavelength of the bulk vibration, and the second-order thickness shear (TS2) mode, in which the bulk vibration is perpendicular to the thickness direction and one acoustic wavelength is contained in the piezoelectric layer thickness, are denoted in the figure. This 20 type of dispersion, in which the TE1 mode has increasing  $k_{\parallel}$  with increasing frequency, is called Type 1. Type 1 materials include, e.g. ZnO. Aluminum nitride is inherently Type 2 (in Fig. 4b, TE1 mode is the lower dispersion curve, and TS2 mode is the upper dispersion curve), but with an appropriate design of the acoustic Bragg reflector, the resonator structure's dispersion can be tailored to be of Type 1.

25

In Fig. 4b, positive values of  $k_{\parallel}$  denote real wave number (propagating wave) and negative values correspond to imaginary wave number (evanescent wave). For a resonance to arise, the acoustic energy must be trapped inside the resonator structure. In the thickness direction, isolation from the substrate (mirror or air gap) ensures the energy trapping. In the 30 lateral direction, there should be an evanescent wave outside the resonator region for energy trapping. Energy trapping is possible between frequencies  $f_{o1}$  and  $f_{o2}$ . Frequency range for which energy trapping occurs for the TE1 mode,  $f_{o2}-f_a$ , is shaded in Fig. 4b. Energy trapping is easier to realize in Type 1 dispersion. Therefore, when using AlN as the

piezoelectric material, the mirror is usually designed so that it converts the dispersion into Type 1. This limits somewhat the design of the acoustic mirror.

As the lateral wave number  $k_{\parallel}$  increases on a dispersion curve (lateral wavelength decreases), lateral standing wave resonances (plate modes) appear in the resonator structure. For a plate mode to arise, the width of the resonator  $W$  must equal an integer number of half wavelengths of the plate mode:

$$W = N \frac{\lambda_m}{2}$$

10

for the mode  $m$  with wavenumber  $k_m = 2\pi/\lambda_m$ .

### Acoustical coupling in BAW devices

15 A filter can be made by electrically connecting one-port resonators to form a ladder or a lattice filter. Another possibility is to arrange mechanical (acoustic) coupling between resonators by placing them close enough to each other for the acoustic wave to couple from one resonator to another. Such devices are called coupled resonator filters (CRF).

20 In BAW devices, vertical acoustic coupling between stacked piezoelectric layers is used in stacked crystal filters (SCF, see Fig. 5(a)) and vertically coupled CRFs (Fig. 5 (b)). In an SCF, two piezoelectric layers are separated by an intermediate electrode. In a vertically coupled CRF, coupling layers are used to modify the coupling strength between the piezo layers. The CRF can be fabricated either using the SMR or the air-gap technology.

25

A thin-film vertically coupled CRF has been shown to give a relatively wide-band frequency response (80 MHz at 1850 MHz center frequency, or 4.3% of center frequency, Fig. 8(a) from G.G. Fettinger, J. Kaitila, R. Aigner and W. Nessler, “Single-to-balanced Filters for Mobile Phones using coupled Resonator BAW Technology”, Proc. IEEE Ultrasonics Symposium, 30 2004, pp. 416-419) with the capability of unbalanced-to-balanced (balun) conversion. The disadvantage of the vertically coupled CRFs is the need for a large number of layers and

their sensitivity to the thickness of the piezolayers. This makes the fabrication process difficult and consequently expensive.

5 Lateral acoustical coupling in BAW (LBAW) can be realized with 2 or more narrow electrodes placed on the piezoelectric layer 1 (Fig. 6) on a thin layer structure 4, in such a way that the acoustic vibration can couple in the lateral direction from one electrode to another. Electrical input signal in Port 1, 5 is transformed into mechanical vibration via the piezoelectric effect. This vibration couples mechanically across the gap to Port 2, 6 and creates an output electrical signal. Electrodes in this example are interdigital (comb-like).

10 Coupling strength is determined by the acoustic properties of the structure and by the gap between the electrodes.

15 Bandpass frequency response is formed by two laterally standing resonance modes arising in the LBAW structure, as illustrated in Fig. 7 for a two-electrode structure. In the even mode resonance, both electrodes vibrate in-phase, whereas in the odd mode resonance their phases are opposite. For a Type 1 resonator, the even mode, having a longer wavelength, is lower in the frequency than the shorter-wavelength odd mode. The frequency difference between the modes determines the achievable bandwidth of the filter, and depends on the acoustic properties of the structure and on the electrode dimensions.

20

Vertical CRF's have disadvantages as they are difficult and costly to fabricate, i.e. they require several layers and are sensitive to piezoelectric films' thickness.

25 LBAW is therefore advantageous because it has a simple fabrication process and the operation frequency is mainly determined by the piezolayer thickness, though to a lesser extent by electrode geometry. So far however, the obtained bandwidth has been too narrow, i.e. 2%-3% of the center frequency.

30 One problem with LBAW filters is the gently sloping edges of the pass band, which can limit the area of application of the components. By steepening the sloping edges, the competitiveness of LBAW filters would improve significantly.

## SUMMARY OF THE INVENTION

It is an object of the present invention to provide a wide-band acoustically coupled bulk acoustic wave (BAW) filter based on thin-film technology and piezoelectric thin films.

5

An aspect of embodiments of the present invention is that the filters are operable in the GHz frequency range.

More specifically, the filter according to the invention is characterized by what is stated in  
10 the characterizing portion of Claim 1.

Considerable advantages are gained with the aid of the invention. Examples of advantages which can be obtained through embodiments of the invention are as follows.

Wide frequency bandwidth at GHz frequencies is possible. At least in some embodiments, the frequency bandwidth is better than that of known acoustic wave components.

15

The invention also has embodiments, in which there is the possibility to operate the filter at high frequencies, e.g. 1-5 GHz. As frequency is determined mainly by film thicknesses, this means that lithography is not necessarily a principal limiting factor, as it is for SAW components.

20

Further advantages achievable by means of at least some embodiments are the relatively simple fabrication process, e.g. established BAW process with only one piezoelectric layer, compared to competing coupled-resonator BAW technologies, comparatively small component size compared to, e.g. SAW and ladder BAW components, and high out-of-  
25 band suppression compared to, e.g. ladder BAW filters.

It is a further objective of one or more embodiments of the present invention to offer a solution relating to the steepening of the stop-band attenuation of LBAW filters.

30

Also, some embodiments provide a solution permitting a steep stop-band farther from the pass band and taking up much less space than known solutions. This is possible, at least in part, due to the simpler construction presented herein. There is additionally provided a solution permitting balun operation and a change in impedance from one port to another.

According to an embodiment, there is disclosed a bandpass filter with wide (e.g. 5% relative to center frequency) passband which is achieved using lateral acoustic coupling between piezoelectric bulk acoustic wave (BAW) resonators. The device is preferably designed such that one bulk wave mode, e.g., first-order longitudinal thickness mode, is 5 used to produce the passband. With the correct design of the acoustic and electric properties, a bandwidth comparable to or wider than that of the current known acoustic filter components, i.e. surface or bulk acoustic wave, SAW / BAW devices, is obtained at GHz frequencies, e.g. 1-5 GHz.

Some of the benefits of the embodiments are achieved by adding an acoustic resonator or 10 resonators in series or in parallel with the filters. Thus, by using the operating frequency of the resonator it is possible to create a deep dip in the frequency response of the filter which both increasing the steepness of the edges of pass band and stop-band attenuation in the vicinity of the pass band.

There are several applications in which such possibilities are of benefit. The addition of a 15 zero above and/or below the pass band steepens the edges of the pass band and improves stop-band attenuation. With the aid of parallel resonance in parallel resonators and series resonance in series resonators, pass-band attenuation can be reduced, or bandwidth increased.

It is then preferable to select the frequencies in such a way that a parallel resonator 20 produces a zero below the pass band, and a series resonator produces a zero above the band. The stop-band attenuation in LBAW resonators increases as one moves farther from the pass band, whereas in ladder filters, for example, it decreases or remains the same at a level determined by the capacitances of the resonators.

Furthermore, a LBAW filter can implement a balun functionality inside a filter, without a 25 separate component. A balun filter with a steep pass band and a simple manufacturing process is herein possible. Resonators also act as matching elements for an LBAW filter. Compared to pure ladder resonators, which have a steep band, embodiments of the present invention differ in the type of acoustic coupling and the filter construction. A LBAW plus resonators can take up less space, as fewer resonators are needed and stop-band attenuation 30 far from the pass band is better.

## BRIEF DESCRIPTION OF THE DRAWINGS

In the following, the invention is described with the aid of examples and with reference to  
 5 the accompanying drawings:

Fig. 1: (a) Schematic of a SAW device, (b) schematic of a SAW interdigital transducer.

Fig. 2: (a) Solidly-mounted BAW resonator, (b) air-gap BAW resonator.

10 Fig. 3: Schematic of electrical connection of resonators in (a) T-section, (b) Pi-section. (c)  
 5-pole / 2-section ladder filter. There is no acoustic connection between the resonators.

Fig. 4: (a) bulk mode propagation for two bulk modes (longitudinal and shear), (b)  
 15 Schematic picture of dispersion curves of a BAW resonator.

Fig. 5: Schematic illustration of (a) a stacked crystal filter, (b) vertical SMR-type BAW  
 20 CRF.

Fig. 6: Schematic of a two-electrode SMR LBAW structure.

25 Fig. 7: (a) Schematic illustration of the operation principle of a 2-electrode LBAW. The  
 two plate modes (even and odd) create a 2-pole filter response (b).

Fig. 8: Examples of electrical response of a vertically coupled CRF. In the example,  
 20 minimum insertion loss is 1 dB and the 3-dB bandwidth in (a) is ~80 MHz (4.3% at 1850  
 MHz center frequency).

Fig. 9: Microscope image of a 31-electrode LBAW designed and fabricated at VTT.  
 30 Electrode width  $W=2 \mu\text{m}$ , gap width  $G=2 \mu\text{m}$ , electrode length  $L=200 \mu\text{m}$ .

Fig. 10: Dispersion curves calculated for the electrode region of the example filter. TE1  
 cutoff frequency is ~1850 MHz. TS2  $k=0$  frequency ~1780 MHz.

Fig. 11: Dispersion curves calculated for the outside region of the example filter stack. TE1 cutoff frequency is  $\sim$ 1935 MHz. TS2 k=0 frequency is  $\sim$ 1808 MHz.

Fig. 12: Measured electrical frequency response of a 31-electrode LBAW filter designed  
5 and manufactured at VTT. Post-measurement (with software) matching to  $120 \Omega$  parallel  
to 5 nH at both ports was used. Center frequency is 1988 MHz, minimum insertion loss is  
2.1 dB, and relative 3-dB bandwidth is 97 MHz (4.9% of center frequency).

Fig. 13: Connection of resonators to an LBAW filter as a schematic diagram and a circuit  
10 diagram.

Fig 14: Simulated frequency response for a resonator.

Fig 15: Simulated frequency response for a two-finger LBAW filter (black), a parallel  
resonator in the input (dark grey), parallel and series resonators in the output (light grey).

Fig 16: Simulated frequency response for a two-finger LBAW filter (black), a parallel  
15 resonator in the output (dark grey), parallel and series resonators in the output (light grey).

Fig 17: Simulated frequency response for a two-finger LBAW filter (black), parallel and  
series resonators in the input as well as a parallel resonator in the output (dark grey),  
parallel and series resonators in the input and in the output (light grey).

Fig 18: Simulated frequency response for a nine-finger LBAW filter.

20 Fig 19: Simulated frequency response for a nine-finger LBAW filter which has series and  
parallel resonators in the input (dark grey) and in the output (light grey).

Fig 20: Simulated frequency response for a nine-finger LBAW filter, the stop-band  
attenuation of which improves as the frequency moves away from the pass band.

The filter described herein is based on the SMR LBAW structure shown in Fig. 6. Electrodes in this example are interdigital (comb-like), although other geometries, e.g. circular, are possible as well.

5 The LBAW filters according to example embodiments are designed to operate in the first-order thickness-extensional TE1 mode. This is because many piezoelectric thin film materials have electromechanical coupling stronger in the thickness direction, meaning that the longitudinal vibration couples efficiently to the electrical excitation which is over the thickness of the piezoelectric layer.

10

Based on an exemplary demonstrator filter described below, an example structure for creating a wideband response is characterized by:

A BAW structure comprising an acoustic Bragg mirror **4**, electrodes and piezoelectric layer. While the piezoelectric material used in the example is AlN, other 6mm symmetry group piezoelectrics, such as ZnO, can be used as well. Furthermore, thin-film forms of other piezoelectric materials, such as known SAW materials like LiNbO<sub>3</sub>, LiTaO<sub>3</sub>, can be used. The BAW structure is further characterized in that it has Type 1 dispersion.

15 The filter structure has interdigital electrode structure with two ports, in this case metal although other conductive materials can be used, with electrodes **5** and **6** deposited on the thin-film piezoelectric layer. The electrode structure is designed such that the electrodes are connected alternating to port 1 (input) **2** and port 2 (output) **3**.

20 In an embodiment, the number of electrodes **5** and **6** is 31 in total. Their width is 3  $\mu\text{m}$ , the gap between electrodes is 2  $\mu\text{m}$ , and the length of the electrodes is 200  $\mu\text{m}$ .

25 From the sake of clarity, the different regions of the layer stack having top metal will be referred to as the electrode region. The region that has no top metal and is outside of the electrodes is referred to as the outside region.

According to an embodiment, the thin-film layer stack is designed as follows. The mass loading by top the electrode, determined by the top electrode thickness and material

density, is such that the frequency difference between the  $k_{\parallel}=0$  frequency of the electrode region's TE1 mode and the outside region's TS2 mode is small. More particularly, such that the  $k_{\parallel}=0$  frequency of the outside region's TS2 mode is 95%-99% of the electrode region's TE1 cutoff frequency. In the present example the  $k_{\parallel}=0$  frequency of the outside region's TS2 mode is 97.3%.

The frequency difference between the outside region's TS2 and TE1 modes'  $k_{\parallel}=0$  frequencies is designed to be large, e.g. 5%-15% of the electrode region's TE1 mode cutoff frequency. The frequency difference in the present example has been designed to be 6.7%.

Another feature that has to be designed appropriately is the electrode topology. The electrode topology should be designed such that the gap width  $G$  ensures good coupling at the even mode. For example, at least for the most common applications, the gap width should be designed to be 20%-120%, preferably 25%-110% of the evanescent acoustic wave's decay length, i.e. the length at which amplitude  $A = A_0 * 1/e$  of the original amplitude  $A_0$ , in the gap at the desired even resonance mode.

Although an SMR type structure is used in the present example, the present invention is not limited to that type of structure. Other structures such as air-gap structures can be used as well, as long as the acoustic properties are designed appropriately.

Additionally, other bulk vibration modes besides the TE1 can be utilized. However, the piezoelectric coupling of the driving electric field to the used bulk acoustic mode should preferably be strong enough so that low losses can be obtained.

Alternatively, gap width  $G$  can be determined normalized to the piezolayer thickness  $d$ . For example,  $G$  can be designed to be 25%-200% of  $d$ . In the present example  $G$  is designed as 102% of  $d$ .

Electrode width  $W$  is designed such that multiple half-wavelengths cannot fit within the electrode width. For example,  $W$  is designed to be smaller than the lateral acoustic wave's wavelength  $\lambda_{\text{odd}}$  at the desired odd resonance mode.

The number of electrodes N, electrode width W and gap width G are designed such that the desired wavelength of the lateral acoustic wave at the even mode resonance frequency is achieved. That is,  $N*W+N*G=\lambda_{\text{even}}/2$ , where  $\lambda_{\text{even}}$  is the wavelength of the lateral acoustic wave at the even mode resonance frequency. For the present example: N=31, W=3 and 5 G=2. Additionally, the total width of the structure N\*W+N\*G is such that the highest-order mode trapped in the structure is the desired odd mode resonance.

The electrode width W is designed such that the wavelength of the lateral acoustic wave at the desired odd mode resonance frequency,  $\lambda_{\text{odd}}$ , is obtained. For example: W=25%-50% of 10  $\lambda_{\text{odd}}$ .

The tables 1-3 below define acceptable thickness ranges for thin-film layers according to typical embodiments of the present invention. The piezo layer thickness d (minimum and maximum value) is first determined with respect to the acoustic wavelength in the piezo 15 material ( $\lambda$ ) at the operation frequency  $f$ . Thicknesses (min and max) of top electrode (tope), bottom electrode (bote) and the topmost mirror layer (M1) are then defined with respect to the piezo layer thickness. Tope, bote and M1 are labeled in the general schematic of Figure 6(a). The mirror layers underlying the topmost mirror layer M1 are designed such that the required wave reflectivity is obtained. A starting point can be, for 20 example, a thickness that equal one quarter of the acoustic wavelength in the material.

Device operation is dependent on the combination of these layer thicknesses. Therefore the thicknesses are not independent. More than one layer may contribute to one acoustic or dispersion property, and one layer may also contribute to several properties.

**Table 1: Wide range layer thickness percentage**

Layer	Typical material	Symbol	Min, % of $\lambda$	Max, % of $\lambda$	Min, % of d	Max, % of d
Piezo	AlN	d	23	50		
Top electrode	Al	tope	0,8	7,5	3,4	22
Bottom	Mo	bote	1,3	20	5,7	40

electrode						
Top mirror	SiO2	M1	9,7	35	42	70

**Table 2: Medium range layer thickness percentage**

Layer	Typical material	Symbol	Min, % of $\lambda$	Max, % of $\lambda$	Min, % of d	Max, % of d
Piezo	AlN	d	27	41		
Top electrode	Al	tope	1,3	4,2	4,9	10,3
Bottom electrode	Mo	bote	3,1	1189	11,4	29
Top mirror	SiO2	M1	12,7	25,8	47	63

**Table 3: Tight range layer thickness percentage**

Layer	Typical material	Symbol	Min, % of $\lambda$	Max, % of $\lambda$	Min, % of d	Max, % of d
Piezo	AlN	d	30	37		
Top electrode	Al	tope	1,7	3,5	5,7	9,5
Bottom electrode	Mo	bote	4,5	7,0	15	19
Top mirror	SiO2	M1	15	21,5	50	58

Table 3 is representative of the present example. When the piezo layer thickness is chosen to be 1960 nm (35% of  $\lambda$ ) as in the present example, the different ranges provide the following layer thicknesses (in nm) in tables 4-6:

**Table 4: Wide range layer thickness values**

Layer	Typ. material	Thickness min (nm)	Thickness max (nm)
piezo	AlN	1960	
tope	Al	67	294
bote	Mo	112	784
M1	SiO <sub>2</sub>	823	1372

5

**Table 5: Medium range layer thickness values**

Layer	Typ. material	Thickness min (nm)	Thickness max (nm)
piezo	AlN	1960	
tope	Al	96	202
bote	Mo	223	568
M1	SiO <sub>2</sub>	921	1235

**Table 6: Tight range layer thickness values**

Layer	Typ. material	Thickness min (nm)	Thickness max (nm)
piezo	AlN	1960	
tope	Al	112	186
bote	Mo	294	372

M1	SiO2	980	1137
----	------	-----	------

Once the design is chosen, it is determined if matching to the system impedance level is achieved. The design, i.e. N, W, and electrode length, is then modified when necessary, such that matching to the system impedance level is achieved while retaining a desired loss level within the passband.

5 1.

Steepness of passband edges can be improved by adding, in parallel and/or in series, resonators before and/or after the filter.

## 10 Example Filter with Measurement Results

One exemplary example is described herein along with the corresponding measurement results from the example filter. The structure of the filter will now be described below.

15 The filter of the present example consists of a thin-film stack. The nominal thin-film layer thicknesses of the acoustic stack are set forth in Table 7, from bottom to top. The substrate of the filter in the example is silicon. The electrode structure used is interdigital and similar to that shown in Fig. 1(b). A microscope image of the present example is also presented in Fig. 9. The total number of electrodes in 5 and 6 is N=31, the electrode width W=3  $\mu\text{m}$ , the 20 gap width G=2  $\mu\text{m}$ , the electrode length L=200  $\mu\text{m}$  and the probe pad size is 150  $\mu\text{m} \times$  150  $\mu\text{m}$ .

25 Although the electrode and gap width  $W$  and  $G$  are constant in Fig. 1(b) as well as in the component introduced below in Fig. 9, the structure need not be limited to constant  $W / G$  and/or constant period.

**Table 7: Nominal layer thicknesses of the stack in measured devices.**

Layer	SiO2	W	SiO2	W	SiO2	Mo	AlN	Al
Thickness (nm)	790	505	620	510	1030	300	1960	150

Calculated dispersions for the electrode and outside regions are shown in Figs. 10 and 11.

S-parameter measurements were done on-wafer with a vector network analyzer (HP8720D). Measurement was done at  $50 \Omega$  system impedances. As-measured results were matched (in Matlab) after the measurement. Insertion loss  $IL=20\log10(|S21|)$  is plotted in Fig. 12.

5

Within the frequency range of 1-5 GHz, the bandwidth at 2 GHz was found to be 5%. This is compared to 4% at 2GHz of the closest prior art version. Therefore, an increase of 25% bandwidth is realized in the present example. One of ordinary skill in the art will immediately recognize the advantage such an increase in bandwidth at 2 GHz represents to

10 the state of the art.

Furthermore, when looking at the required pattern resolution at 2 GHz, the present example critical dimension was greater than  $1 \mu\text{m}$ . Compared to a standard SAW coupled resonator filter at 2 GHz which has a required critical dimension of around  $0.5 \mu\text{m}$ , there is

15 seen an over 100% increase in resolution requirement using this embodiment.

A second example is presented herein with ZnO as the piezoelectric material. The thin-film stack of this example filter is shown in Table 8.

20

**Table 8: Layer thicknesses in the second example device from bottom to top.**

Layer	SiO <sub>2</sub>	W	SiO <sub>2</sub>	W	SiO <sub>2</sub>	Mo	ZnO	Al
Thickness (nm)	746	654	746	654	746	300	d=1100	200
% of d					67	27	d=32% of $\lambda$	18

The simulated matched passband width obtained with the example stack of Table 8, number of electrodes  $N=31$ , electrode width  $W=6 \mu\text{m}$  and gap with  $G=3 \mu\text{m}$  is 90 MHz at 1933 MHz center frequency (4.7%).

25

Another example is obtained by replacing the mirror stack of the previous example (Table 8) with an air gap. That is, all layers below bottom electrode (Mo) are removed. The

simulated matched bandwidth obtained with  $N=11$ ,  $W=6 \mu\text{m}$  and  $G=3 \mu\text{m}$  is 114 MHz at 1933 MHz (5.9%).

### Modifying Steepness of Passband Edges

5

A laterally acoustically coupled filter (LBAW) has several advantages over ladder filters consisting of separate resonators. These advantages include smaller size, better stop-band attenuation, the possibility to implement a change from a balanced signal to an unbalanced one (balun) without a separate component, as well to modify the impedance level between 10 the ports. However, LBAW filters have by nature gentler pass band edges than, for example, ladder filters, which limits their possible applications.

As can be seen from Figures 13-20, series and/or parallel BAW resonators are used in the input and output to position zeros, i.e. attenuation peaks in the frequency response of the LBAW filter. The frequencies of the attenuation peaks can be determined by altering the 15 mass load of the resonator. For example, altering can be done by etching an AlN layer, growing additional material on top of the resonator or other suitable method known in the art.

It is possible to use various combinations of series and parallel resonators to shape the end response. Furthermore, the device's impedance, i.e. matching, can be adjusted through the 20 size of the resonator.

Figures 13-20 show how the frequency response of an LBAW filter can be shaped with the aid of simple series and parallel resonators. With the aid of zeros set on both sides of the pass band, the edges of the pass band can be steepened while still retaining a good band shape. The resonators also improve stop-band attenuation near to the pass band and act as 25 transmatch circuits.

Figure 13 shows a schematic diagram of a LBAW filter with series and parallel resonators. The most suitable filter combination can be selected for each construction. The filter has a piezoelectric layer **111** supporting, a parallel resonator **112** and a series resonator **113** at the input of a LBAW filter **114**, as well as a series resonator **115** and a parallel resonator 30 **116** at the output of the LBAW filter **114**.

Acoustic series **113**, **115** and/or parallel resonators **112**, **116** can be connected to the input and output. Various combinations of the resonators described are possible. In the parallel resonators **112**, **116** the lower electrode is grounded. In the series resonators **113**, **115** the signal goes to the lower electrode.

5 The following simulations shown in Figures 14-20 are based on an acoustic thin-film stack, the materials and film thicknesses of which (from the substrate upwards) are listed in Table 9 below.

**Table 9: Thin-film pack used in the simulations**

Material	Si	SiO <sub>2</sub>	W	SiO <sub>2</sub>	W	SiO <sub>2</sub>	Ti	Mo	AlN	TiW	Al
Thickness nm	Substrate	786	505	621	507	1029	25	296	1960	17	106

10 The frequency of the series **113**, **115** and parallel resonators **112**, **116** can be altered, in such a way that the resonator's series and parallel resonances will occur at the desired frequencies. The frequency can be adjusted by altering the thickness of one or more thin films. The thickness of the piezoelectric film has been altered by thinning or material can be grown on top of the resonators to form a mass load, in which case the resonance  
15 frequency will decrease.

Figure 14 shows the frequency responses of three BAW resonators, simulated using 1D models. The black curve is the resonance response **121** produced by the stack of Table 1. The light-grey curve **122** corresponds to a frequency-shifted resonator, with an AlN layer that has been thinned to 1900 nm. This resonator is used as the parallel resonator in the  
20 simulations. The dark-grey curve **123** corresponds to a frequency-shifted resonator that has been correspondingly thinned to 1810 nm. This resonator is used as the series resonator in the simulations.

The simulated frequency response in Figure 14 is for a resonator sized 100  $\mu\text{m}$  x 100  $\mu\text{m}$  using the stack (black) of Table 1. The frequency of the series resonance of the  
25 unmodified resonator **121a** is 1815 MHz and the frequency of the parallel resonance **121b** is 1860 MHz. The light-grey and dark-grey curves are the simulated responses for the

frequency-shifted resonators. The series resonance **122a** of the parallel resonator has been shifted to the frequency 1850 MHz, which is below the pass band, so that the parallel resonance **122b** is at the frequency 1900 MHz, i.e. it is on the pass band. The series resonance **123a** of the series resonator is 1905 MHz (on the pass band) and the parallel resonance **123b** is 1960 MHz (above the pass band). The filter's response receives powerful attenuations at the series resonance frequency of the parallel resonator and at the parallel resonance frequency of the series resonator.

Unwanted lateral responses will arise in a real two-dimensional resonator, which 1D simulation does not take into account. To ensure the best response, it would be good to use some structure, which attenuates the lateral resonance shapes, in the resonators. The following simulations present the responses of two different LBAW constructions and the effects of the resonators on the electrical frequency response.

Figure 15 pertains to a two-finger LBAW filter. In the figure, the simulated frequency response of a two-finger LBAW filter based on the stack of Table 1 is shown in black, **131**. The response is matched with an impedance of 500 Ohm. On the right-hand side of the pass band is a zero point produced by the acoustic structure, but the lower edge of the band is very gentle.

If a parallel resonator **112** is added to the input of the construction, i.e. response **122** of Figure 14, a strong attenuation peak, which appears as the dark-grey response **132** in Figure 15, arises at the series-resonance frequency (1850 MHz) below the pass band. Therefore, stop-band attenuation improves by more than 10 dB below the pass band and by about 7 dB above it. As can be seen though, at the same time the bandwidth decreases somewhat.

When a series resonator **113** is also added to the input, i.e. the response **123** of Figure 14, an attenuation peak is obtained at its parallel resonance frequency (1960 MHz). The steepness of the upper edge of the pass band improves and the stop-band attenuation improves by some dB, compared to only a parallel resonator **112**.

Figure 15 uses a black curve to show the resonance response **131** of a two-finger LBAW filter, a dark-grey curve to show the resonance response **132** if there is a parallel resonator in the input of the filter **131**, and a light-grey curve to show the resonance response **133** if there are parallel and series resonators in the input of the filter **131**.

Figure 16 shows the same resonator combinations in the output port. Figure 16 uses a black curve to show the resonance response **141** of a two-finger LBAW filter, a dark-grey curve to show the resonance response **142** if there is a parallel resonator in the output of the filter **141**, and a light-grey curve to show the resonance response **143** if there are parallel and 5 series resonators in the output of the filter **141**. A parallel resonator will have nearly the same effect as in the input port, but a series resonator will create a peak in the response.

Figure 17 shows other possibilities. Figure 17 uses a black curve to show the resonance response **151** of a two-finger LBAW filter, a dark-grey curve to show the resonance response **152** if there are parallel and series resonators in the input and a parallel resonator 10 in the output, and a light-grey curve to show the resonance response **153** if there are parallel and series resonators in both the input and the output.

The best result is achieved if both a series and a parallel resonator are added to the input and a parallel resonator is added to the output. With this configuration band-edge steepness improves considerably. Stop-band attenuation improves below the band by nearly 30 dB 15 and above it by nearly 15 dB. At the same time, the width of the pass band decreases to some extent. In accordance with the present example the decrease is as follows; absolute 5 dB pass band: 55 MHz (2.9 %)  $\rightarrow$  42 MHz (2.2 %) where the percentage is compared to a frequency of 1900 MHz.

The examples according to Figures 18 – 20 deal with a nine-finger LBAW filter. As 20 shown, by increasing the number of fingers the filter's bandwidth can be increased.

Figure 18 uses black to show the simulated frequency response **161** of a 9-finger LBAW filter based on the stack of Table 1 with the response matched by an impedance of  $100 \Omega$ . The bandwidth (abs. 5 dB) is 78 MHz (4.1 %), but both edges of the pass band are very gentle.

25 By adding a parallel resonator, such as with frequency response **122** to the input, the dark-grey frequency-response curve **162** is obtained, in which there is an attenuation peak at a frequency of 1850 MHz. A series resonator with the example frequency response **123** in the input gives the light-grey curve **163**, in which there is an attenuation peak at a frequency of 1960 MHz. Both resonators in the input create the dark-grey curve **164**, in 30 which there are peaks at both frequencies. As can be seen, the upper edge of the pass band is both wider and better shaped, i.e. there is smaller insertion attenuation. The stop-band

attenuation improves below the pass band by about 3 dB and above it by about 2 dB. Unlike a ladder filter, the stop-band attenuation increases as one moves away from the pass band frequency.

In Figure 19, series and parallel resonators in the input and output are compared. Figure 19

5 uses black to show the simulated frequency response **171** of a 9-finger LBAW filter based on the stack of Table 1. Both resonators in the input create the dark-grey curve **172**, in which there are peaks at the frequencies 1850 MHz and 1960 MHz of the previous example as well. On the other hand, the adding of both resonators to the output instead of the input weakens the stop-band attenuation, according to the light-grey curve **173**.

10 Figure 20 uses black to show the simulated frequency response **181** of a 9-finger LBAW filter based on the stack of Table 1. Both resonators in the input create the dark-grey curve **182**, in which there are peaks at the frequencies 1850 MHz and 1960 MHz of the previous example as well. In addition to the above, the addition of a parallel resonator to the output improves the response slightly, according to the light-grey curve **183**. The absolute 5-dB

15 bandwidth of the filter achieved is 77 MHz (4 %). The stop-band attenuation improves as one moves away in frequency from the pass band.

As is seen from figures 14-20, the use of various combinations of resonators allows for the tailoring of LBAW frequency responses. While several combinations of resonators has been shown herein, based on the disclosed description, one of ordinary skill in the art will

20 recognize further combinations, and sub-combinations, which achieve the same or similar goals as the presented combinations without departing from the scope of the invention.

The present invention is not limited to the exemplary examples described herein. The exemplary examples and embodiments merely show some of the advantageous effects of a

25 filter designed according to the present invention. However, one of ordinary skill in the art will recognize obvious variations and combinations of elements described herein which do not part from the scope of the present invention.

Generally, to obtain a filter according to the present embodiments with some or all of the

30 desired, advantageous effects, the following should normally be designed or accounted for in the filter design; correct acoustic properties i.e. dispersion, TE1 mode is trapped in the

structure (outside region preferably has evanescent wave at operation frequency range), maximum frequency difference between even and odd resonance modes, long lateral wavelength at the even mode (long decay length outside the electrodes), high enough Q value for low losses, appropriate electrode design, odd mode is trapped, insuring

5 fabrication tolerances are not critical e.g. not too narrow gaps, matching electrode length and number of electrodes (not too much resistance), choosing small enough component size, insuring no intermediate lateral modes that would produce notches in the passband.

When taking into account some or all of the factors mentioned above, it is possible to

10 produce a filter with extremely wide passband and a simple fabrication process. Wide obtainable band gives freedom to design using wider electrodes and gaps. More electrodes eases the matching to 50 Ohms. The need to use matching inductances or other matching elements is smaller and the requirement to gap width is relaxed allowing for easier fabrication. Better performance (lower losses etc) can be achieved when there is enough

15 bandwidth to sacrifice a portion of the bandwidth.

Other materials besides 6mm symmetry group can be utilized such as thin-film forms of piezoelectric SAW materials e.g. LiNbO<sub>3</sub> and LiTaO<sub>3</sub>. Additionally, operation frequency does not principally depend on electrode dimensions, but on film thicknesses. Therefore

20 high frequency operation is possible and lithography is not a limiting factor.

## CLAIMS:

1. Acoustically coupled thin-film BAW filter, comprising
  - 5 - a piezoelectric layer (1),
  - an input-port (2) on the piezoelectric layer (1) changing electrical signal into an acoustic wave, and
  - an output-port (3) on the piezoelectric layer (1) changing acoustic signal into electrical signal,

10 characterized in that

  - the ports (2, 3) include electrodes (5, 6) positioned such that acoustic coupling is achieved,
  - the filter is capable of operating in the first order thickness-extensional TE1 mode, and
  - wherein the mass loading by the top electrode (plateback) is such that the frequency difference between the  $k=0$  frequency of the electrode region's TE1 mode and the outside region's TS2 mode is relatively small.
2. A filter in accordance with claim 1, characterized in that the  $k=0$  frequency of the outside region's TS2 mode is between 93% and 99.9%, in particular between 95% and 99%, more particularly between 97% and 98% of the electrode region's TE1 cutoff frequency.
3. A filter in accordance with claim 1 or 2, characterized in that the electrodes (5, 6) are positioned such that acoustic vibration in the lateral direction from one electrode to the other acoustically couples the electrodes.
4. A filter in accordance with any previous claim, characterized in that the filter structure that has interdigital electrode structure with two ports, such that the electrodes are connected alternatingly to the input port (2) and the output port (3).

5. A filter in accordance with any previous claim, characterized in that the electrode topology is such that gap width G ensures good coupling at the even mode.
6. A filter in accordance with claim 5, characterized in that the gap width is between 5 20% and 120%, in particular between 25% and 110%, of the evanescent acoustic wave's decay length in the gap at the desired even resonance mode, where the wave's decay length is expressed as the length at which amplitude  $A = A_0 * 1/e$  of the original amplitude  $A_0$ .
- 10 7. A filter in accordance with any previous claim, characterized in that the electrode width W is such that more than one half-wavelength of the lateral acoustic wave's wavelength cannot fit within the electrode width.
- 15 8. A filter in accordance with any previous claim, characterized in that the electrode width W is smaller than the lateral acoustic wave's wavelength  $\lambda_{odd}$  at the desired odd resonance mode.
- 19 9. A filter in accordance with any previous claim, characterized in that the number of electrodes N, electrode width W and gap width G are designed such that the desired wavelength of the lateral acoustic wave at the even mode resonance frequency is achieved.
- 25 10. A filter in accordance with claim 9, characterized in that  $N*W+N*G=\lambda_{even}/2$ , where  $\lambda_{even}$  is the wavelength of the lateral acoustic wave at the even mode resonance frequency, and that the highest-order mode trapped in the structure is the desired odd mode resonance.
- 30 11. A filter in accordance with any previous claim, characterized in that the electrode width W is such that the wavelength of the lateral acoustic wave at the desired odd mode resonance frequency,  $\lambda_{odd}$ , is obtained.

12. A filter in accordance with claim 11, characterized in that W is between 25% and 50% of  $\lambda_{\text{odd}}$ .
13. A filter in accordance with any previous claim, characterized in that matching to 5 the system impedance level is achieved, while retaining a desired loss level within the passband by the combination of N, W, and electrode length L.
14. A filter in accordance with any previous claim, characterized in that the piezoelectric layer (1) is formed on an acoustic Bragg structure (4) formed as a thin 10 film stack or on an air-gap structure.
15. A filter in accordance with any previous claim, characterized by there being one or more resonators added to the filter in parallel and/or series.
16. A filter in accordance with claim 12, characterized in that one or more of the resonators are coupled before and/or after the filter.
17. A method for manufacturing a filter in accordance with any or the previous claims.

20

25

30

## Patenttivaatimukset:

1. Akustisesti kytketty ohutkalvo-BAW-suodatin, joka käsitteää

5

- pietsosähköisen kerroksen (1),

- tulopartin (2) pietsosähköisellä kerroksella (1) sähköisen signaalin muuttamiseksi akustiseksi aalloksi, ja

10

- lähtöportin (3) pietsosähköisellä kerroksella (1) akustisen signaalin muuntamiseksi sähköiseksi signaaliksi,

**tunnettu** siitä, että

15

- portit (2, 3) sisältävät elektrodit (5, 6), jotka on si joitettu siten, että saadaan akustinen kytkentä,

20

- suodatin pystyy toimimaan ensimmäisen kertaluvun pak suusaalton TE1-muodossa, ja

25

- jolloin yläelektrodilla (pinnoitus) saatava massakuorma on sellainen, että taajuusero elektrodialueen TE1-muodon ja ulkoalueen TS2-muodon  $k=0$  -taajuuden välillä on suhteellisen pieni.

30

2. Patenttivaatimuksen 1 mukainen suodatin, **tunnettu** siitä, että ulkoalueen TS2-muodon  $k=0$  -taajuus on 93-99,9 %, erityisesti 95-99 % ja vieläkin erityisemmin 97-98 % elektrodi alueen TE1-rajataajuudesta.

3. Patenttivaatimuksen 1 tai 2 mukainen suodatin, **tunnettu** siitä, että elektrodit (5, 6) on sijoitettu niin, että lateraalisesa suunnassa oleva akustinen värähtely elektrodista toiseen kytkee elektrodit akustisesti.

5

4. Jonkin edeltävän patenttivaatimuksen mukainen suodatin, **tunnettu** siitä, että suodatinrakenteessa on sormilomitettu elektrodirakenne, jossa kaksi porttia on aina niin, että elektrodit on liitetty vuorotellen tuloporttiin (2) ja lähtöporttiin (3).

10

5. Jonkin edeltävän patenttivaatimuksen mukainen suodatin, **tunnettu** siitä, että elektroditopologia on sellainen, että väli G varmistaa hyvän kytkenän parillisessa muodossa.

15

6. Patenttivaatimuksen 5 mukainen suodatin, **tunnettu** siitä, että välin leveys on 20-120 %, erityisesti 25-110 % vaimenvan akustisen aallon vaimenemispituudesta elektrodivälissä halutussa parillisen resonanssin muodossa, jolloin aallon 20 vaimenemispituus ilmaistaan pituutena, jolla amplitudi  $A=A_0 * 1/e$  alkuperäisestä amplitudista  $A_0$ .

25

7. Jonkin edeltävän patenttivaatimuksen mukainen suodatin, **tunnettu** siitä, että elektrodileveys  $W$  on sellainen, että enempää kuin yksi puoliaallonpituus lateraalisen akustisen aallon aallonpituudesta ei sovi elektrodileveyteen.

30

8. Jonkin edeltävän patenttivaatimuksen mukainen suodatin, **tunnettu** siitä, että elektrodileveys  $W$  on pienempi kuin lateraalisen aallon aallonpituus  $\lambda_{pariton}$  halutussa parittomassa resonanssimuodossa.

9. Jonkin edeltävän patenttivaatimuksen mukainen suodatin, **tunnettu** siitä, että elektrodien lukumäärä  $N$ , elektrodileveys  $W$  ja elektrodiväli  $G$  on suunniteltu siten, että saadaan 5 haluttu lateraalisen akustisen aallon aallonpituus parillisen muodon resonanssissa.

10. Patenttivaatimuksen 9 mukainen suodatin, **tunnettu** siitä, että  $N*W+N*G=\lambda_{parillinen}/2$ , missä  $\lambda_{parillinen}$  on lateraalisen 10 akustisen aallon aallonpituus parillisen muodon resonanssi- taajuudella.

11. Jonkin edeltävän patenttivaatimuksen mukainen suodatin, **tunnettu** siitä, että elektrodileveys  $W$  on sellainen, että 15 saadaan lateraalisen akustisen aallon aallonpituus halutulla parittoman muodon resonanssitaajuudella  $\lambda_{pariton}$ .

12. Patenttivaatimuksen 11 mukainen suodatin, **tunnettu** siitä, että  $W$  on 25–50 % aallonpituudesta  $\lambda_{pariton}$ . 20

13. Jonkin edeltävän patenttivaatimuksen mukainen suodatin, **tunnettu** siitä, että saadaan sovitus järjestelmän impedanssiin, samalla kun saadaan pidetyksi tavoiteltu päästökaistan sisäinen häviötaso, arvojen  $N$ ,  $W$  ja elektropituuden  $L$  yhtis- 25 telmän avulla.

14. Jonkin edeltävän patenttivaatimuksen mukainen suodatin, **tunnettu** siitä, että pietosähköinen kerros (1) on muodostettu Braggin rakenteelle (4), joka on muodostettu ohutkal- 30 vopinoksi tai ilmarakorakenteeksi.

15. Jonkin edeltävän patenttivaatimuksen mukainen suodatin, **tunnettu** siitä, että suodattimeen on lisätty yksi tai useampi resonaattori rinnan ja/tai sarjaan.
- 5 16. Patenttivaatimuksen 12 mukainen suodatin, **tunnettu** siitä, että yksi tai useampi resonaattoreista on kytketty suodattimen eteen ja/tai taakse.
- 10 17. Jonkin edeltävän patenttivaatimuksen mukaisen suodattimen valmistamisen menetelmä.

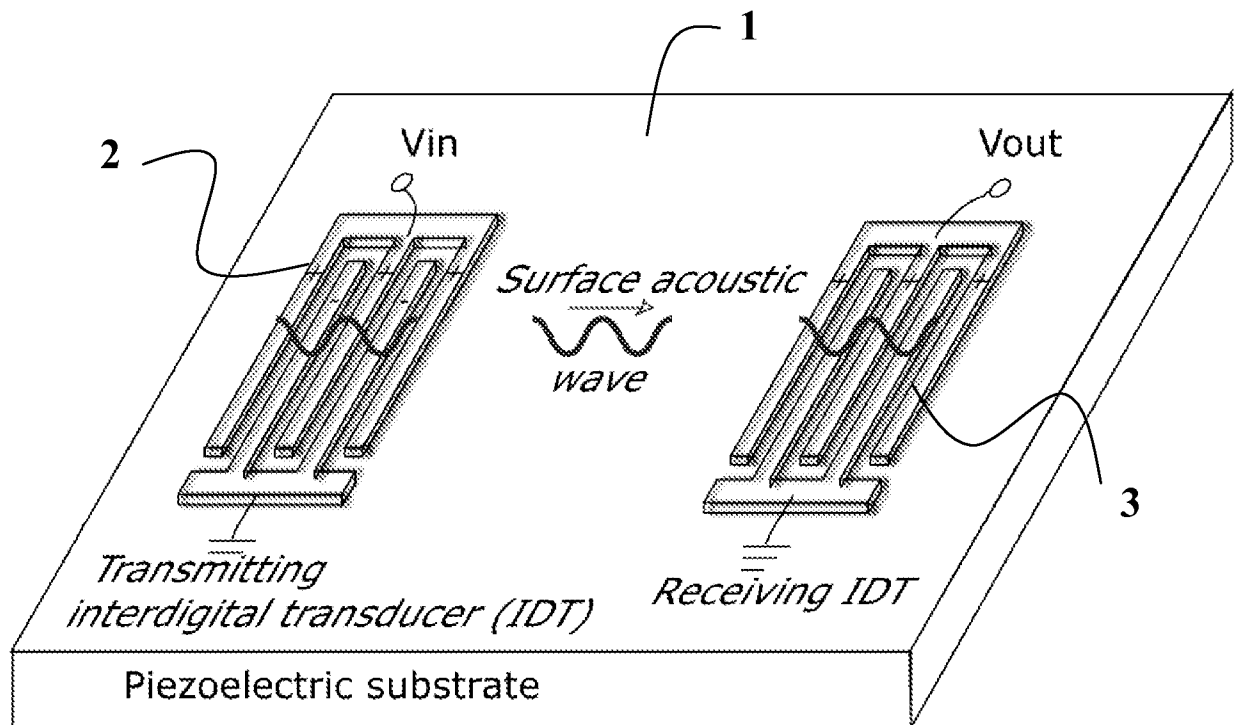


Fig. 1a

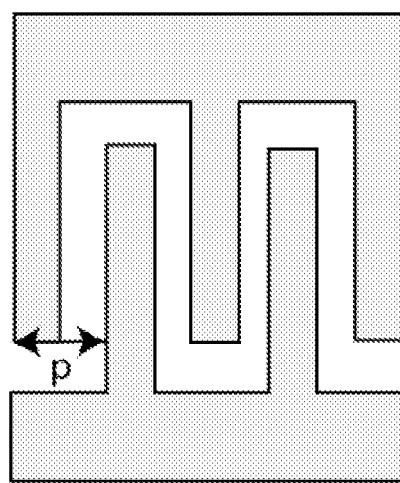


Fig. 1b

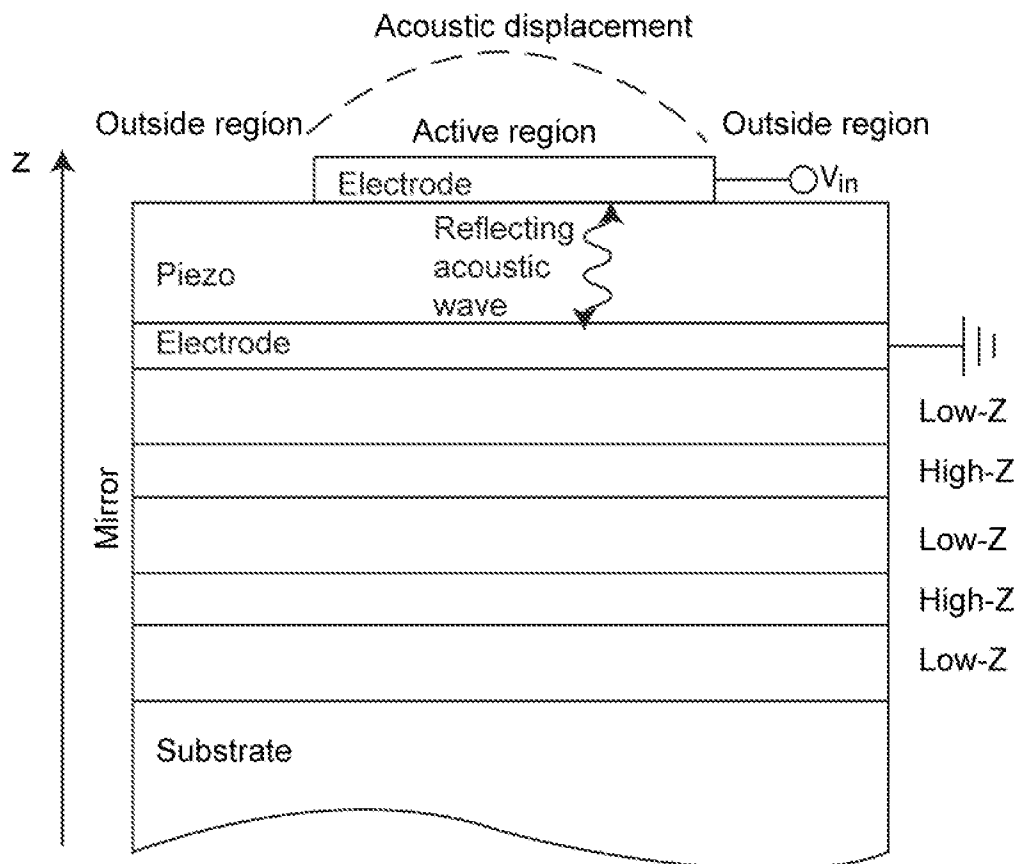


Fig. 2a

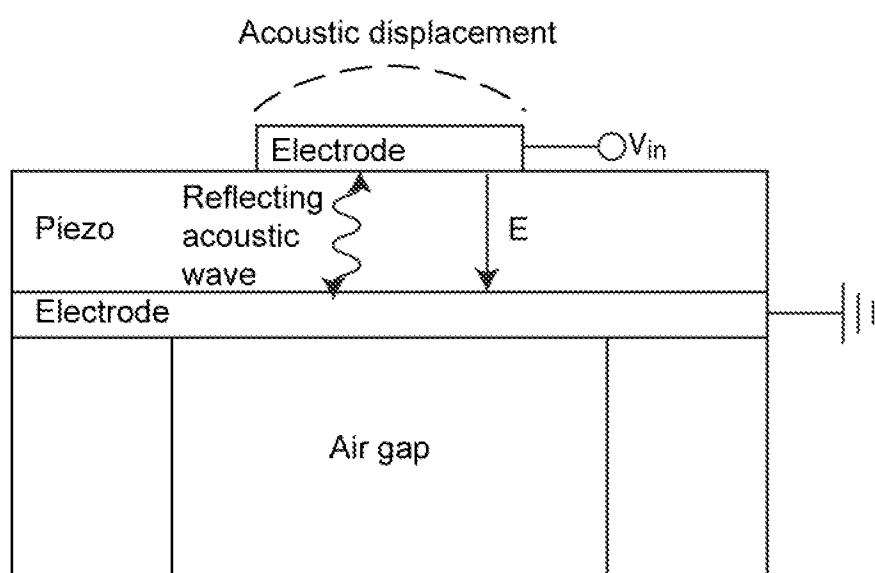
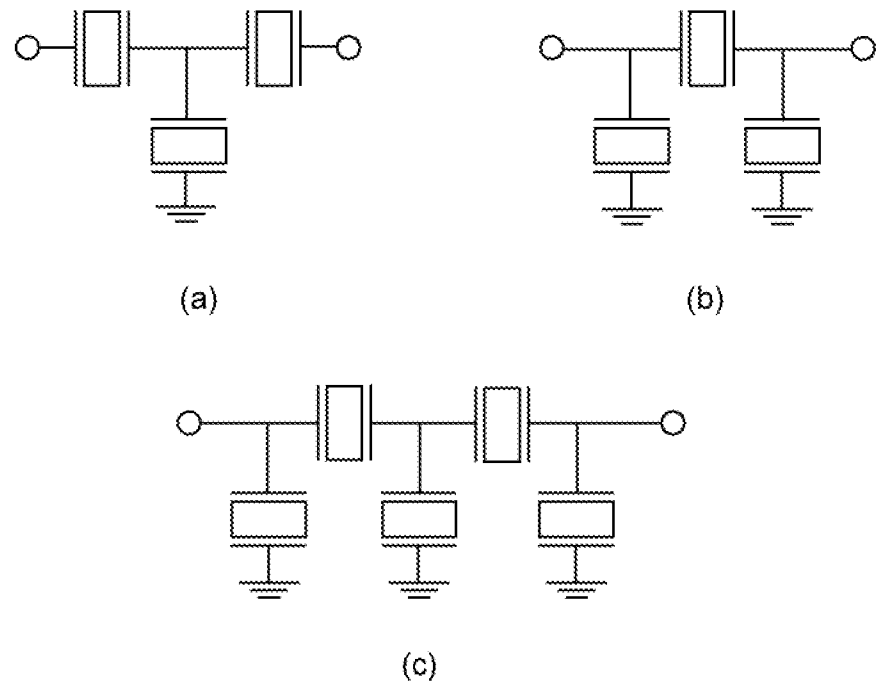


Fig. 2b



**Fig. 3**

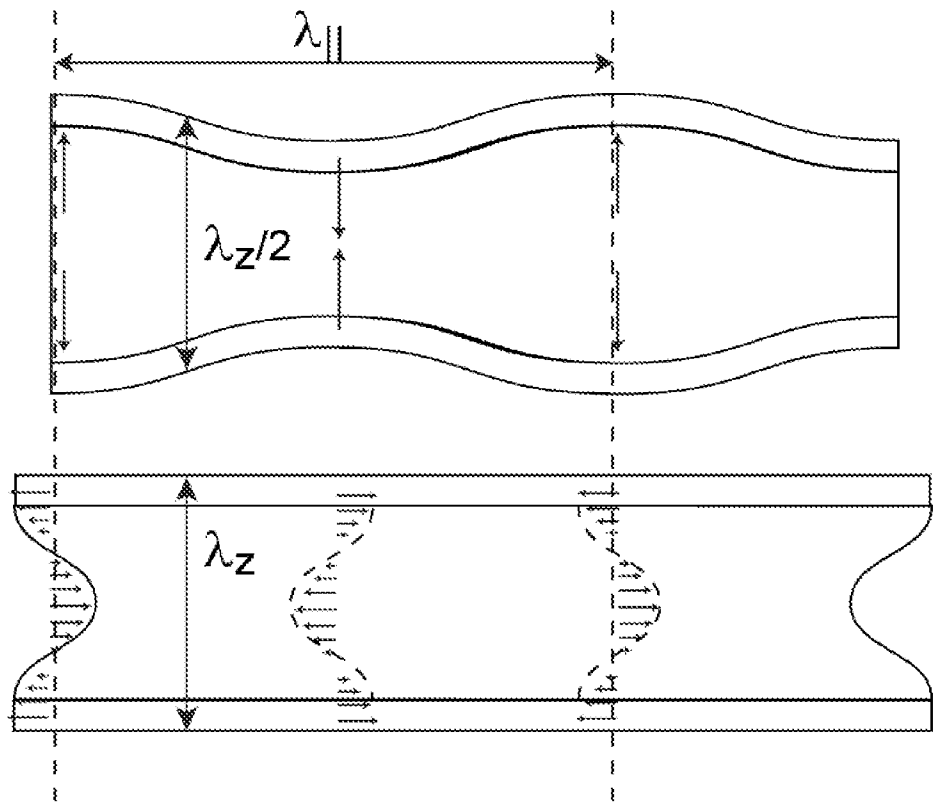


Fig. 4a

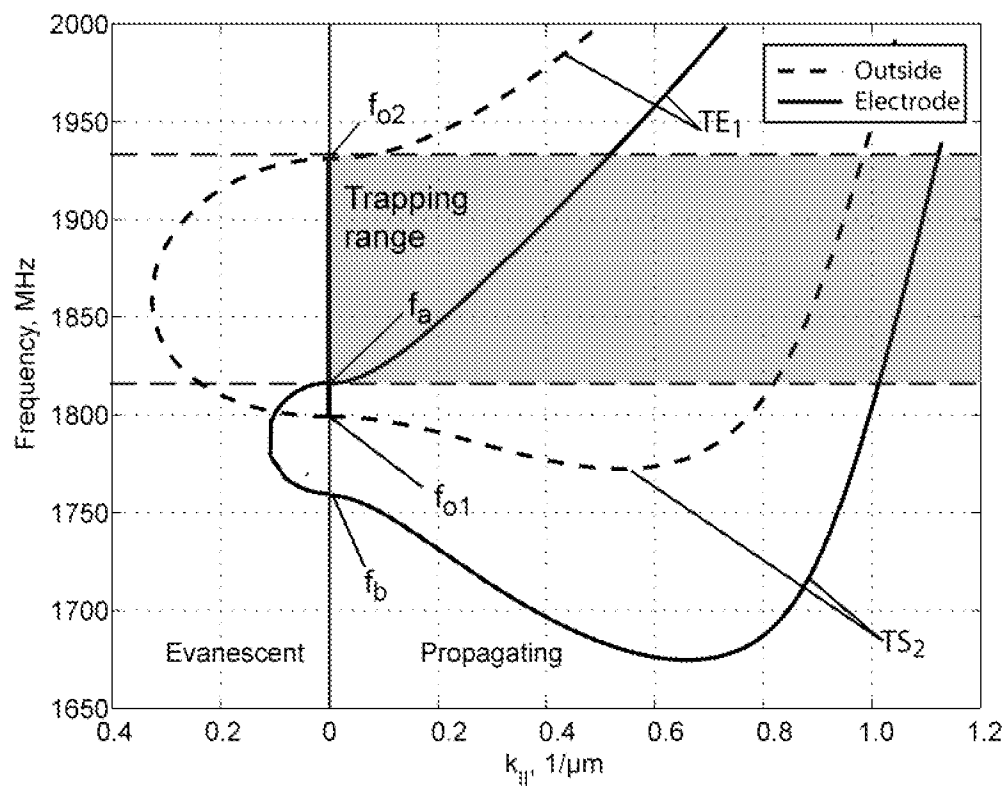
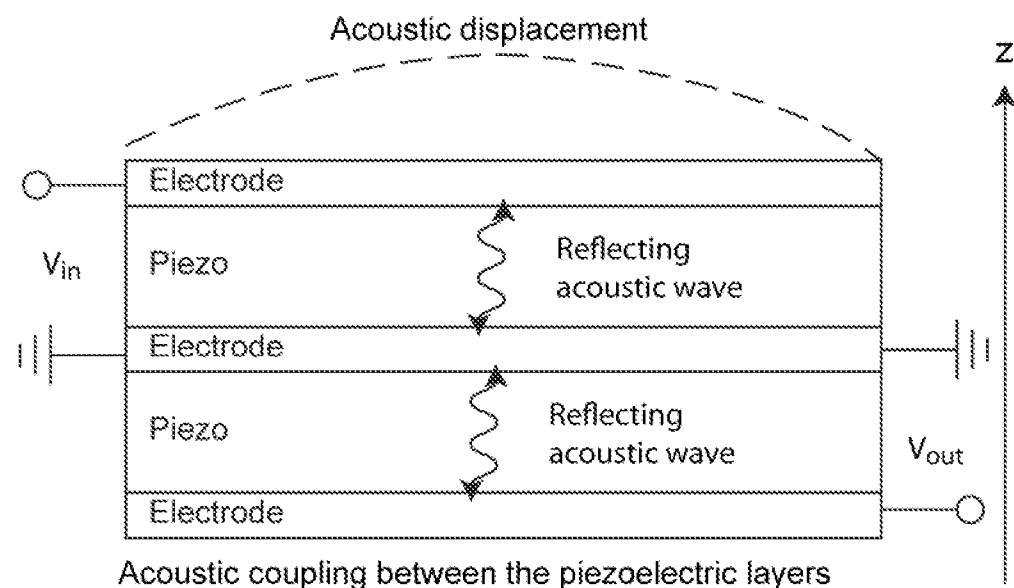
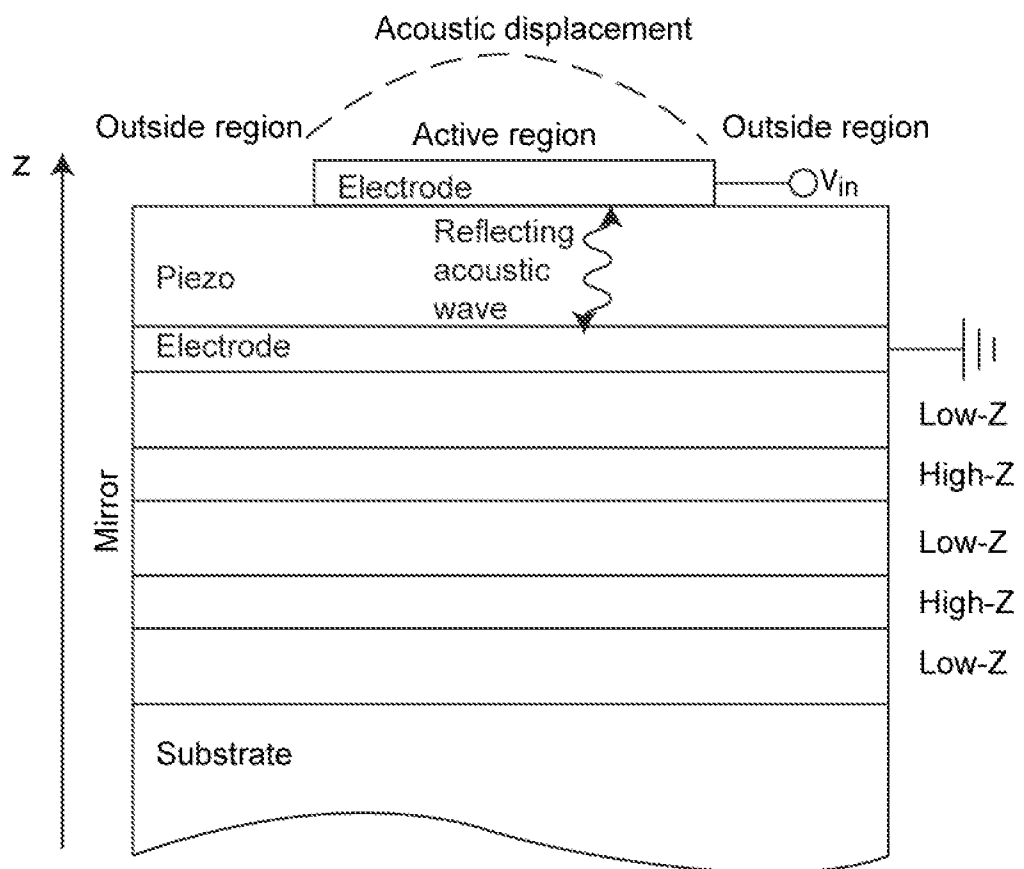


Fig. 4b



**Fig. 5a**



**Fig. 5b**

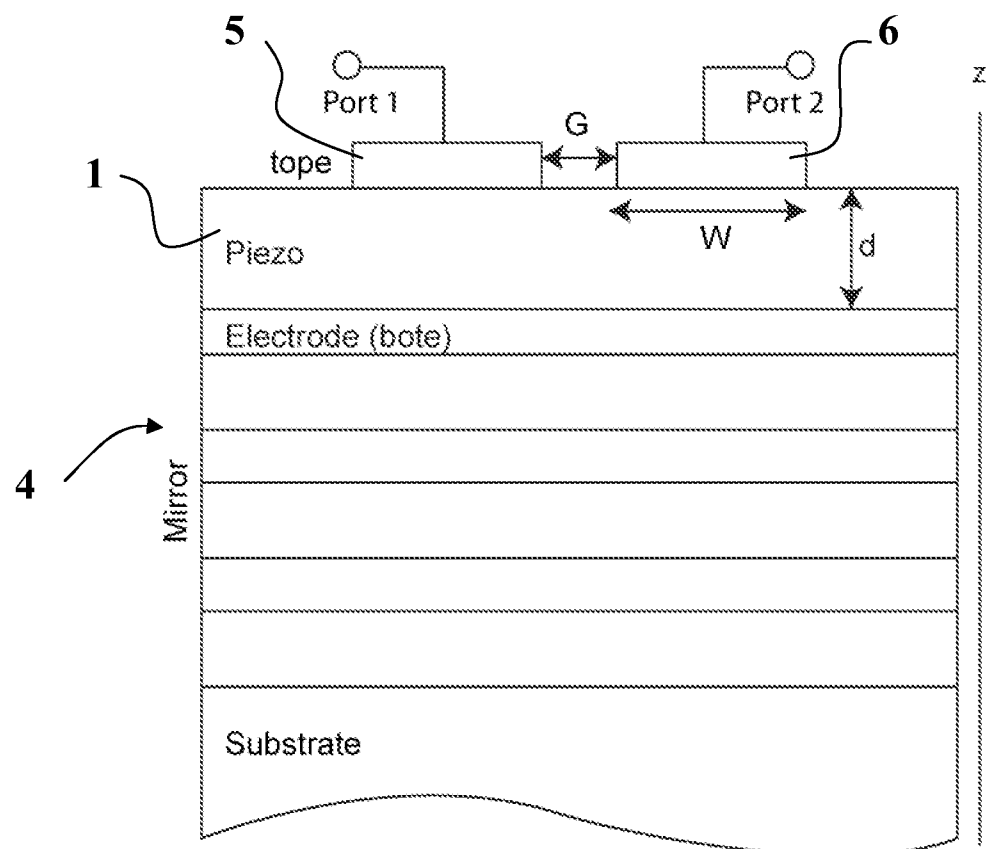


**Fig. 6**

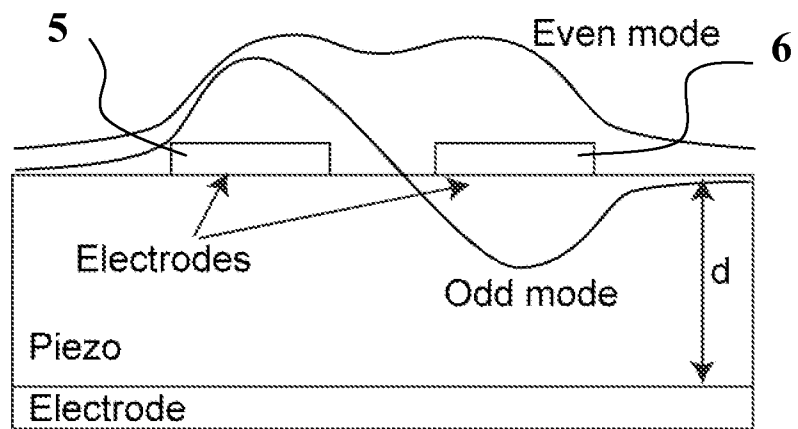


Fig. 7a

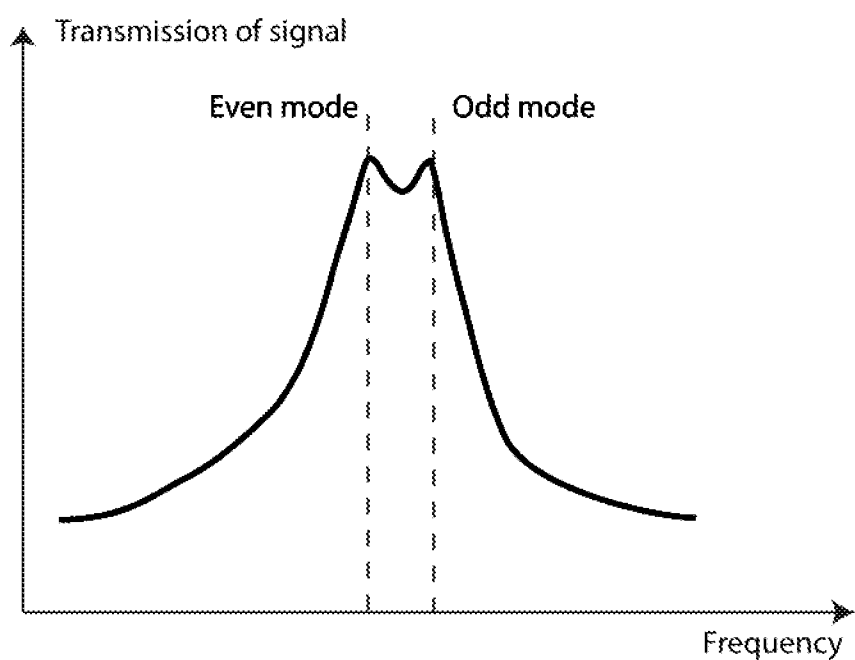
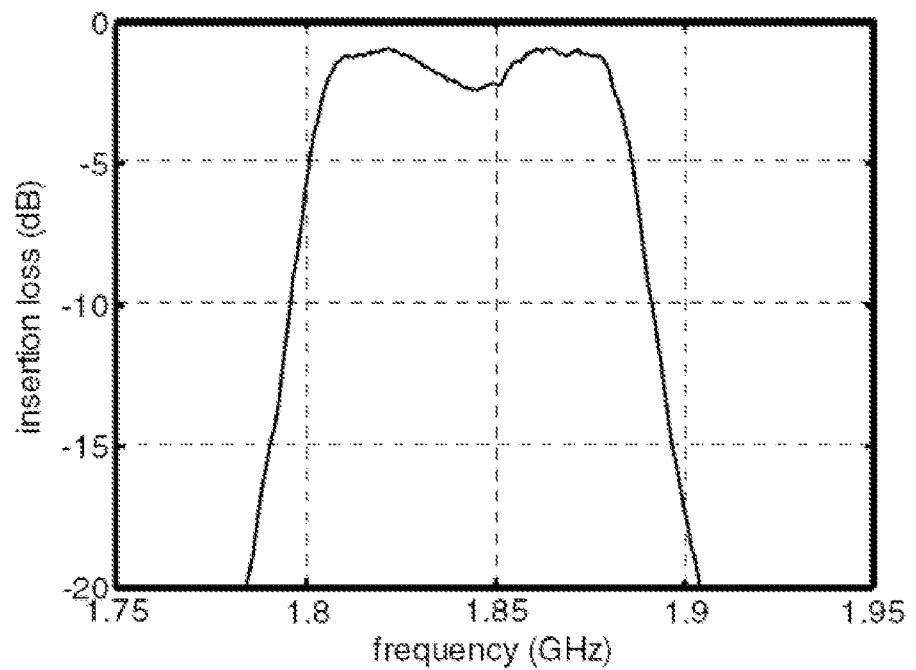
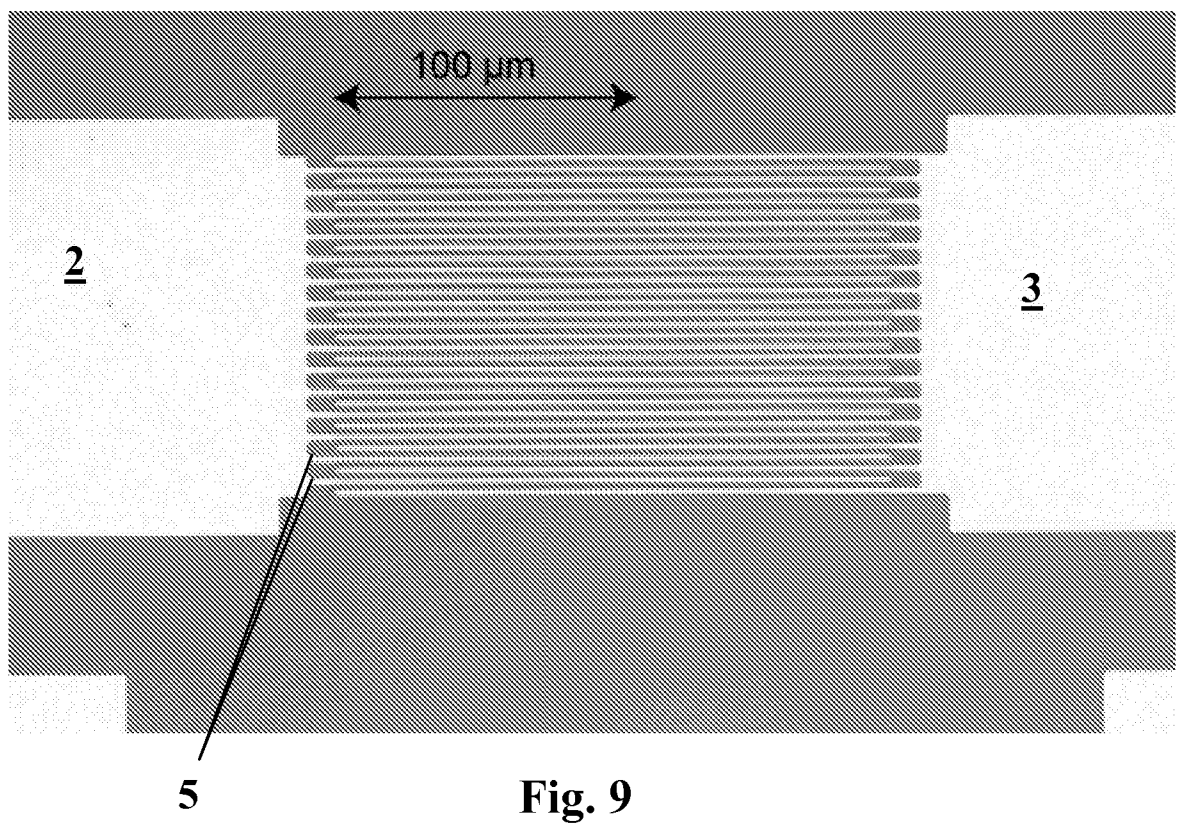


Fig. 7b



**Fig. 8a**



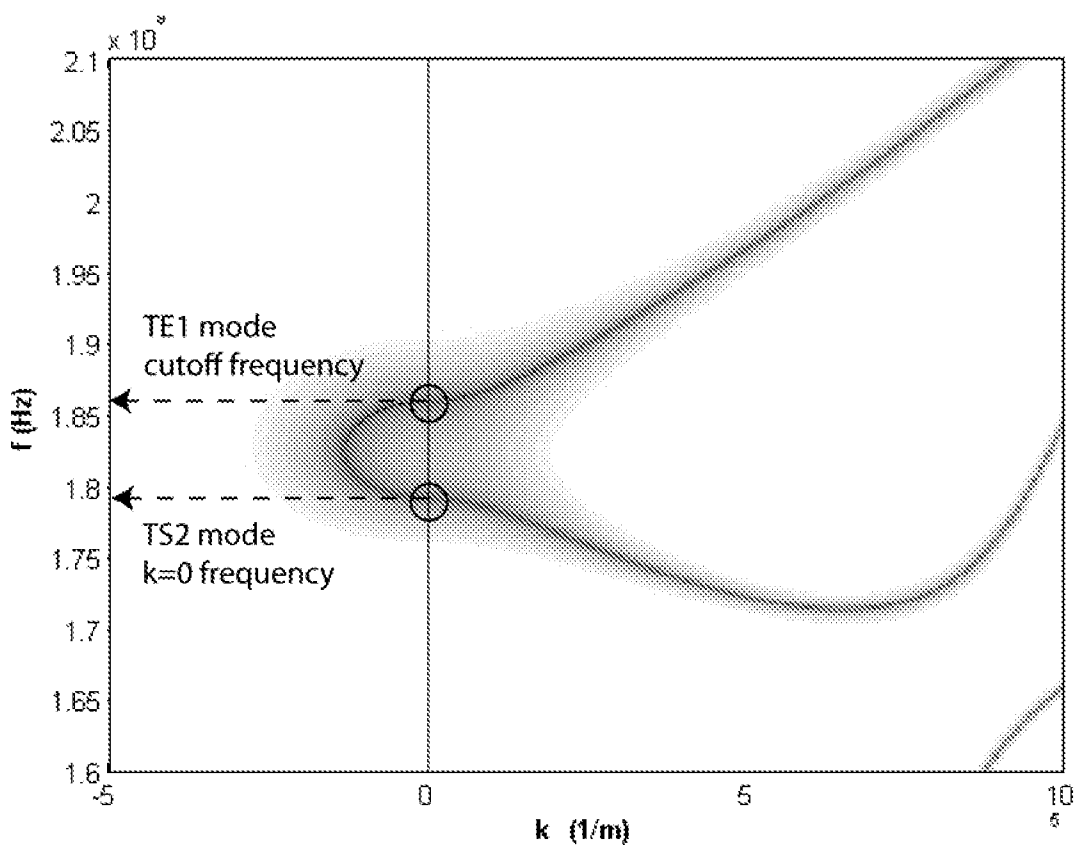
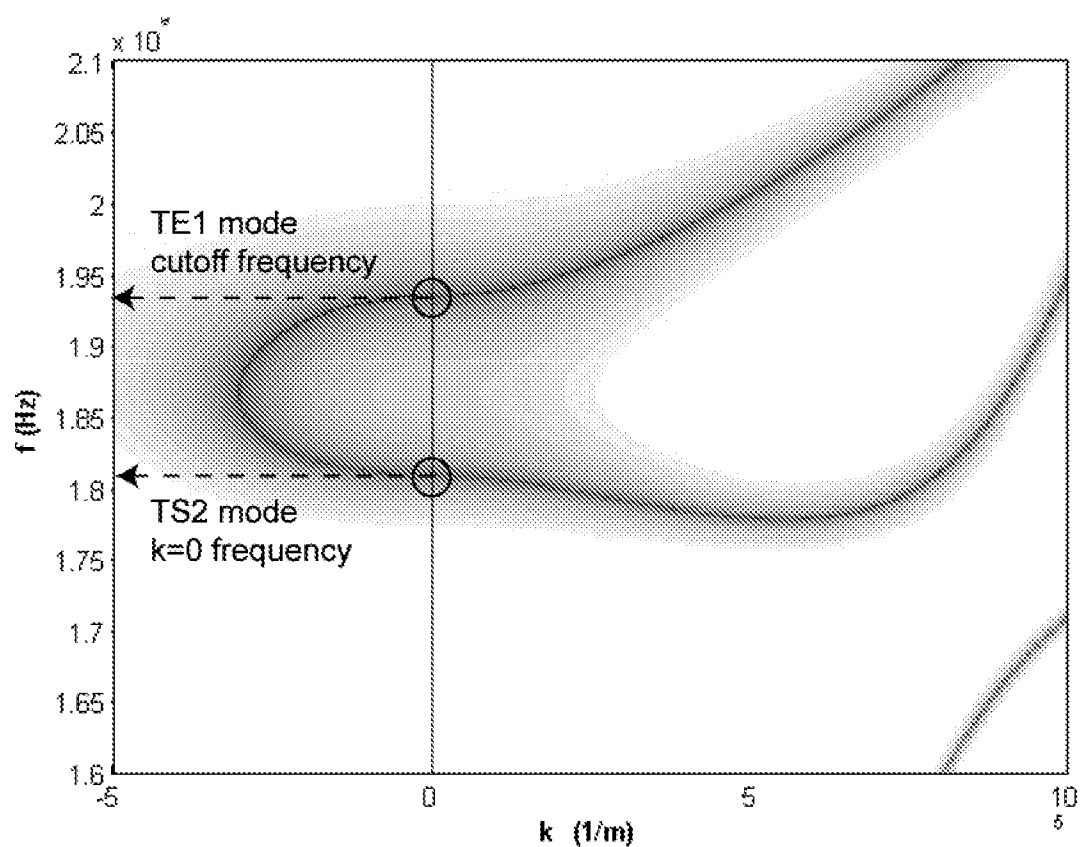
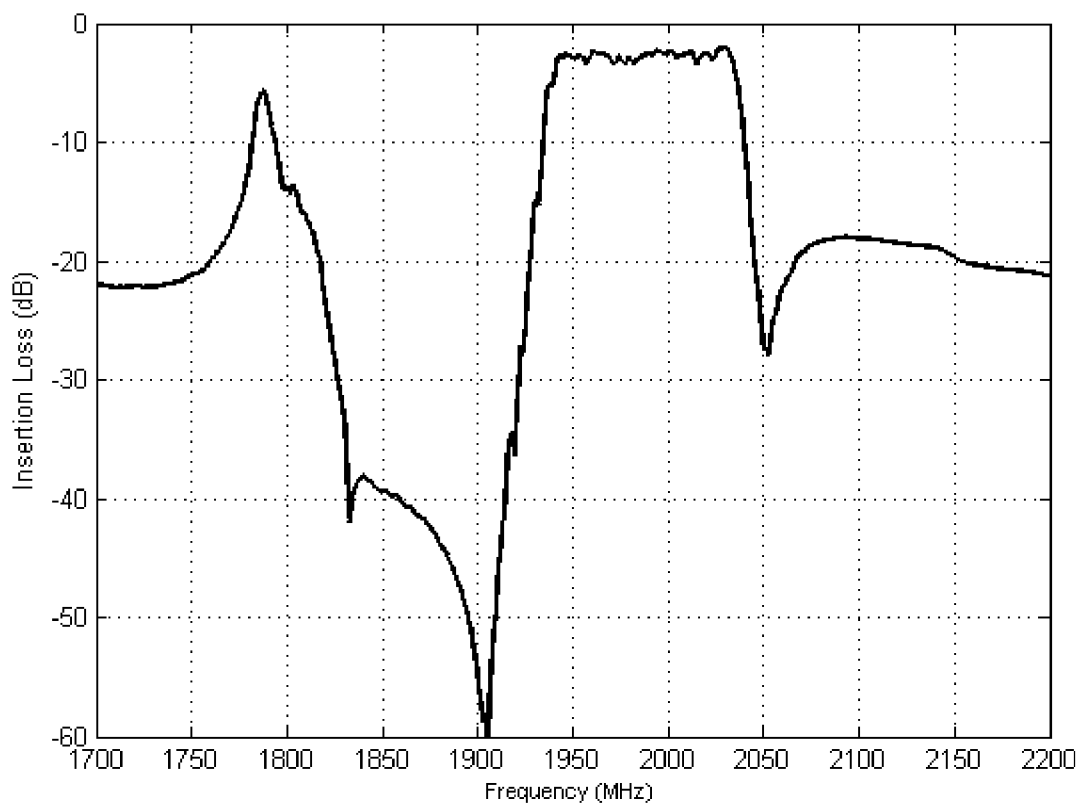


Fig. 10



**Fig. 11**



**Fig. 12**

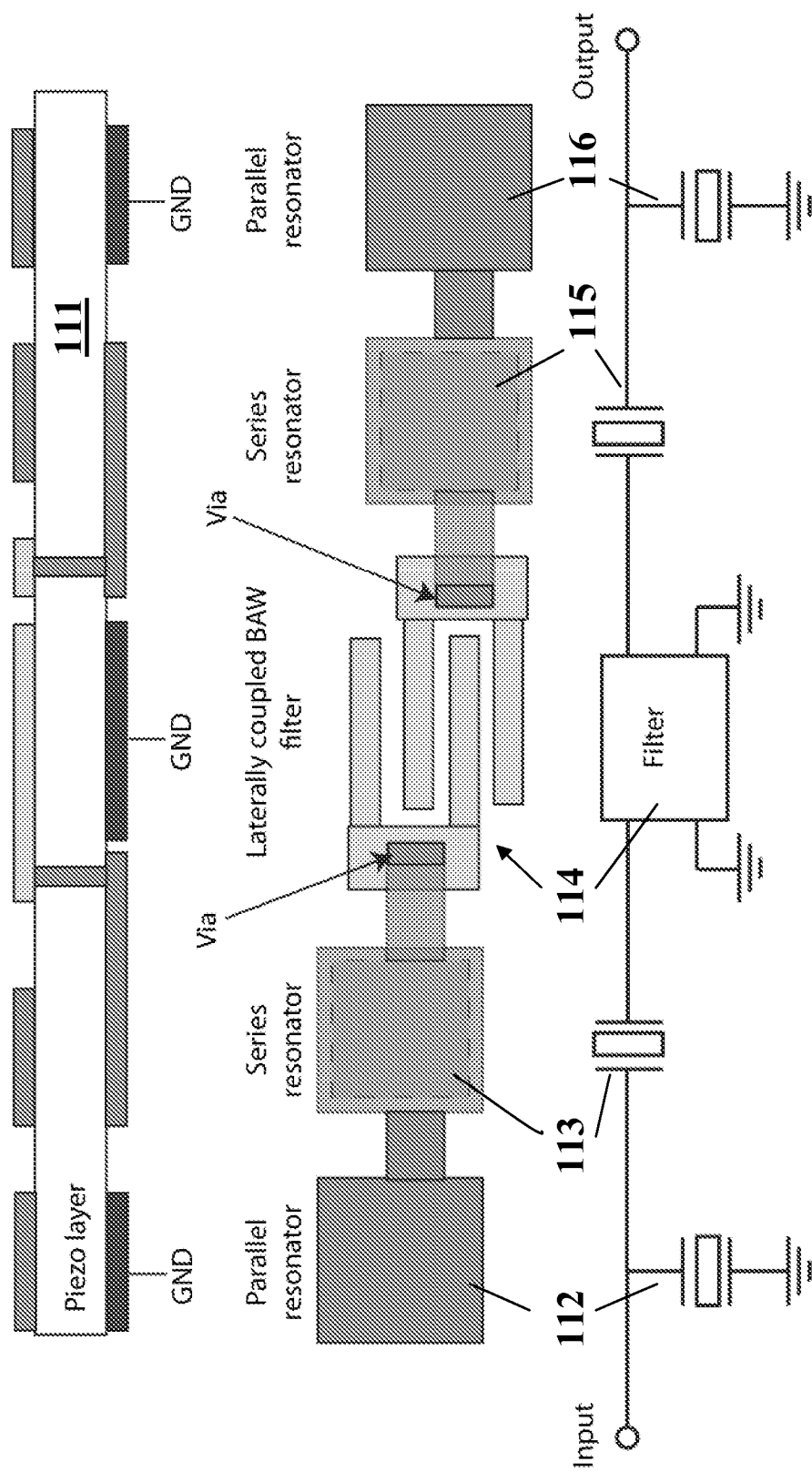


Fig. 13

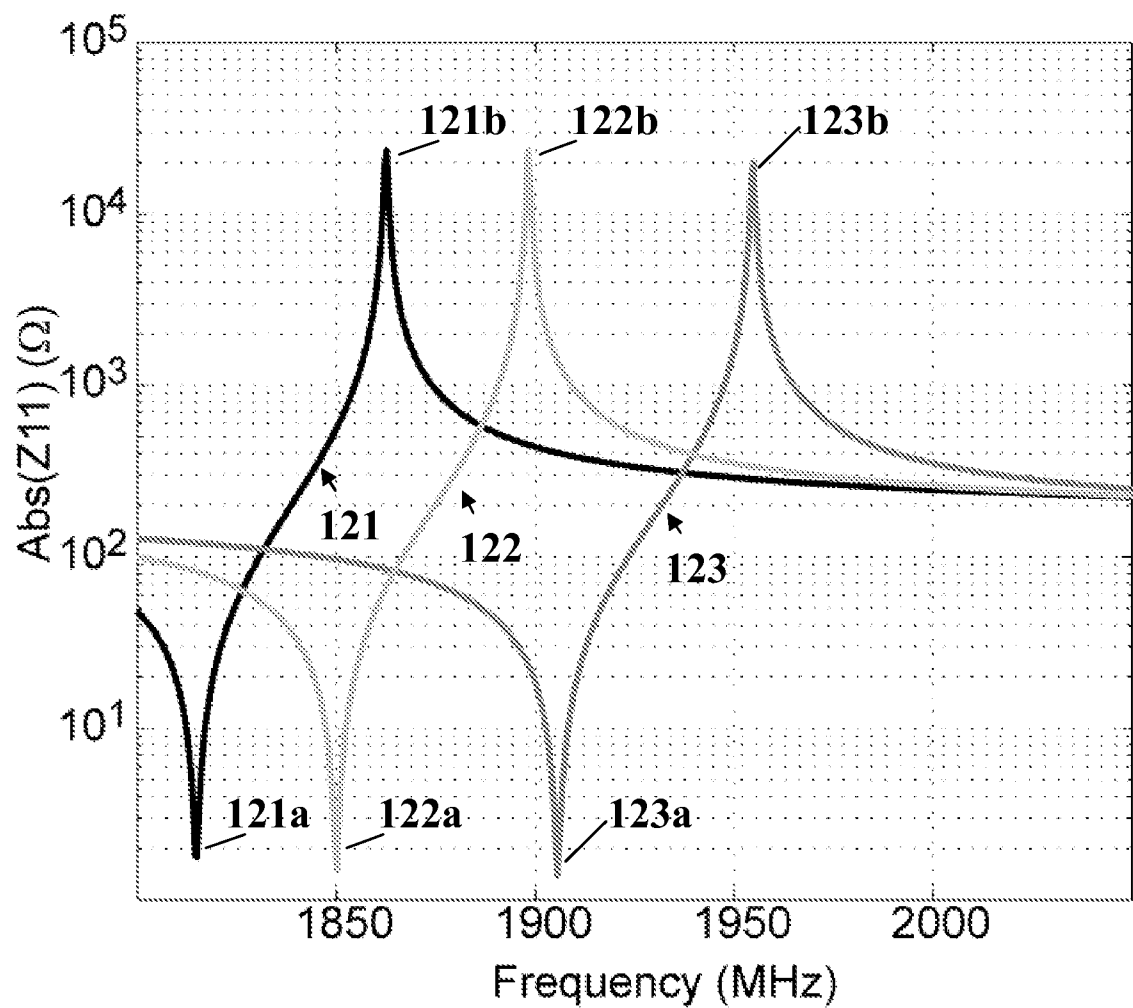


Fig. 14

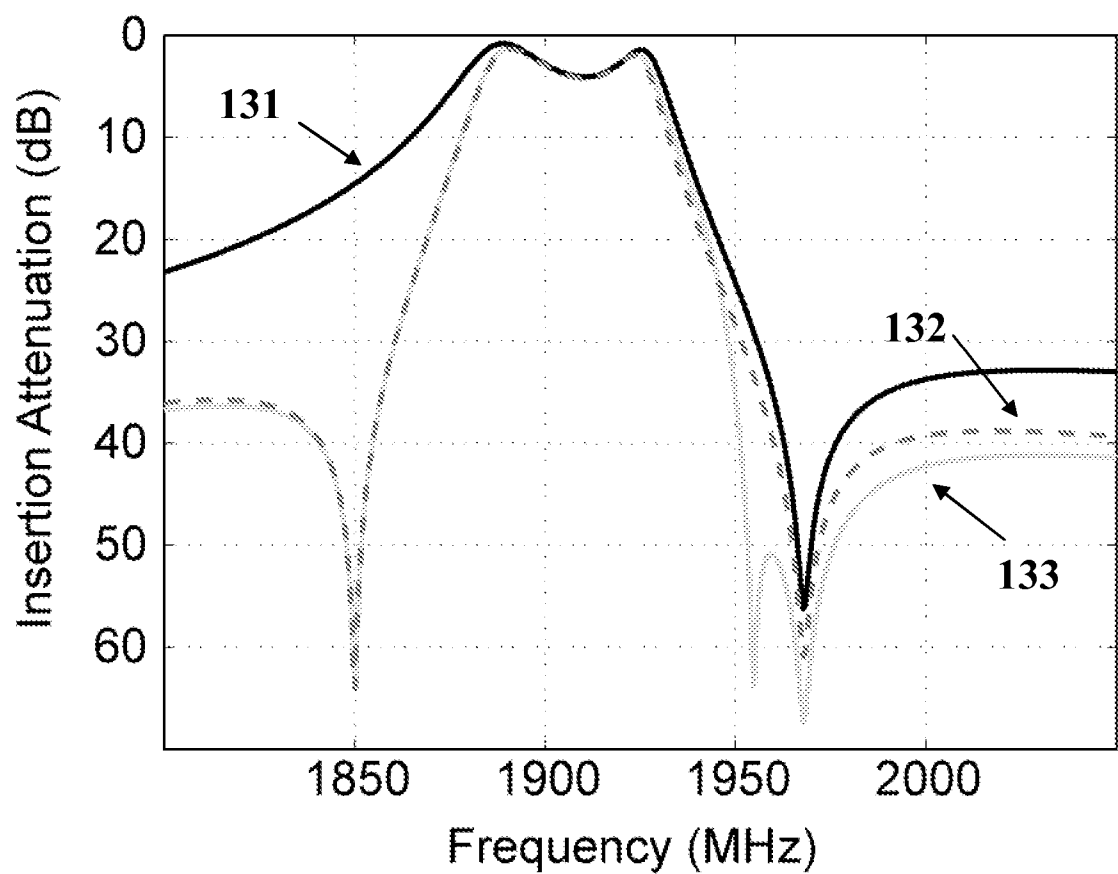


Fig. 15

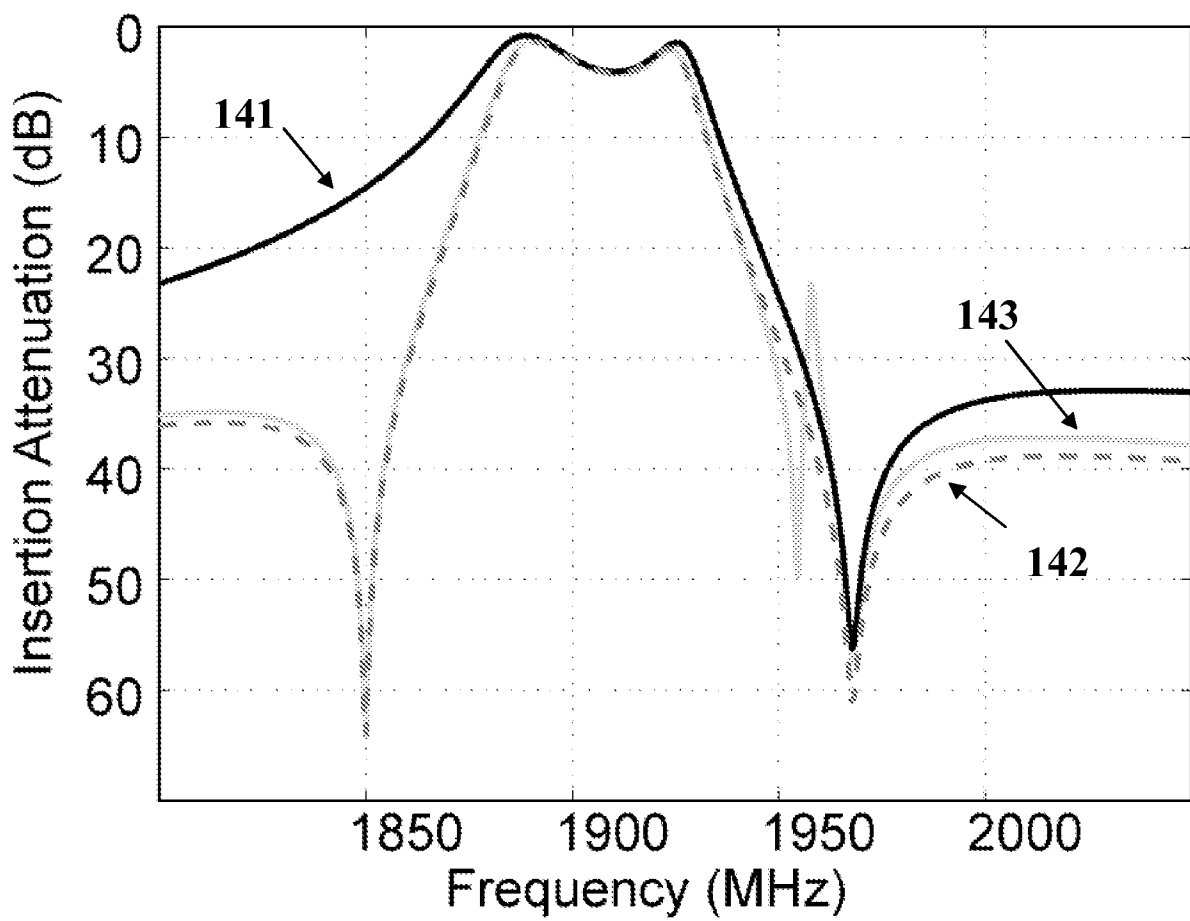


Fig. 16

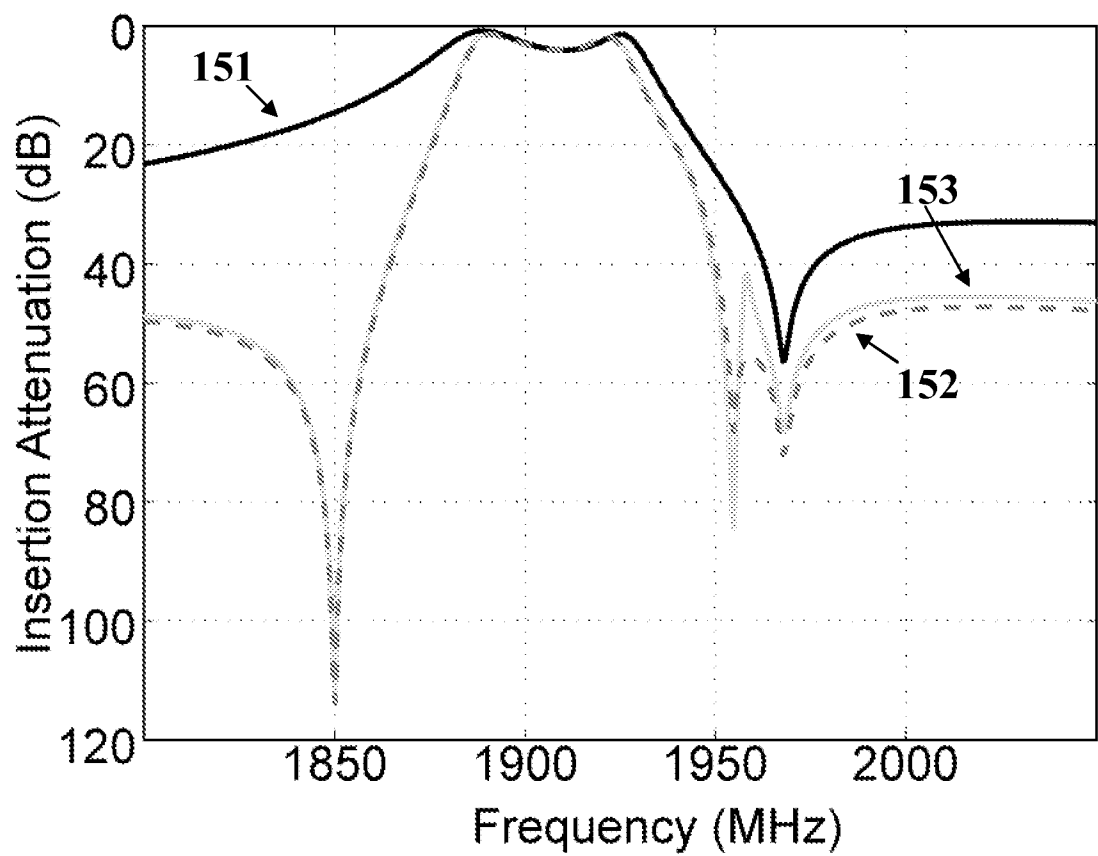


Fig. 17

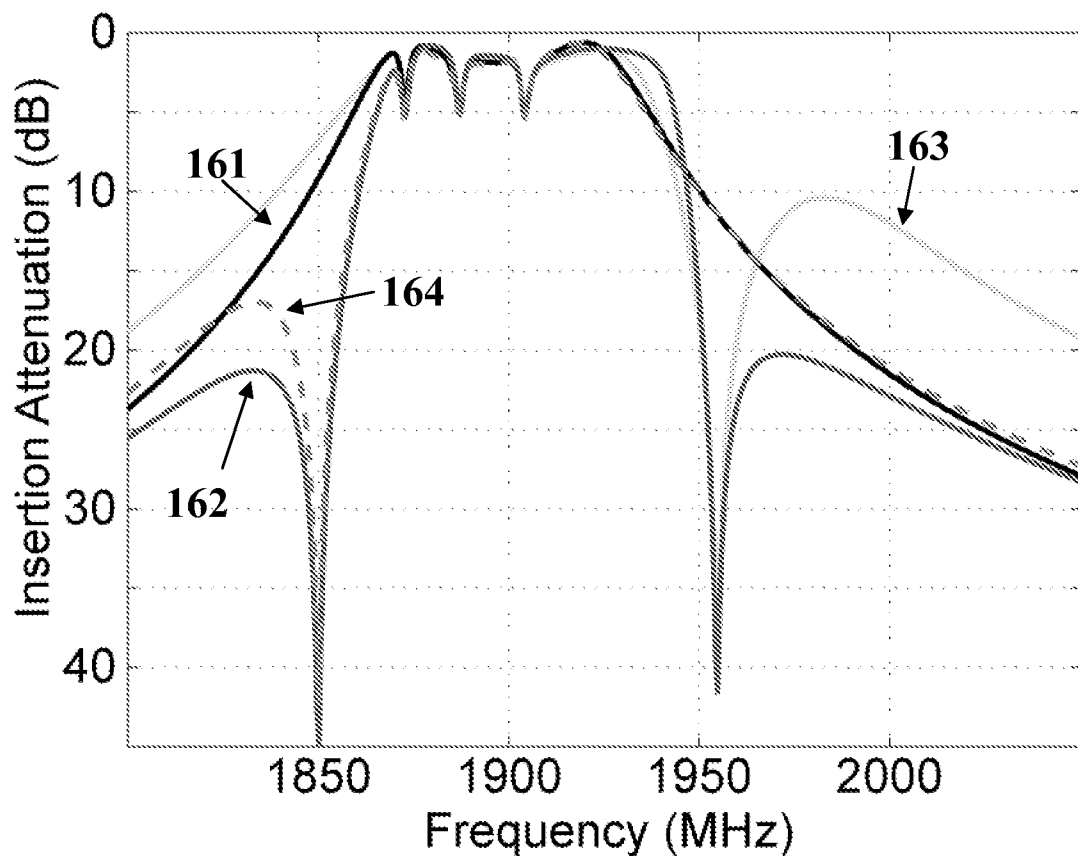


Fig. 18

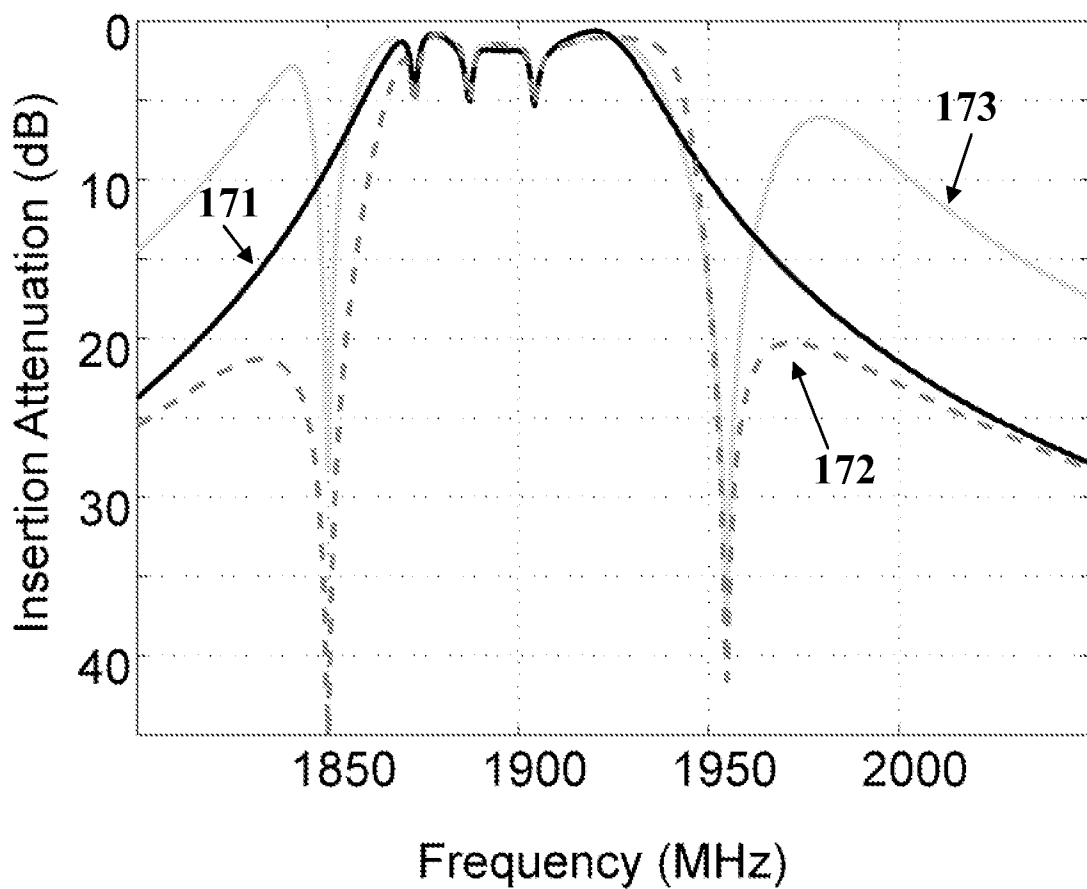


Fig. 19

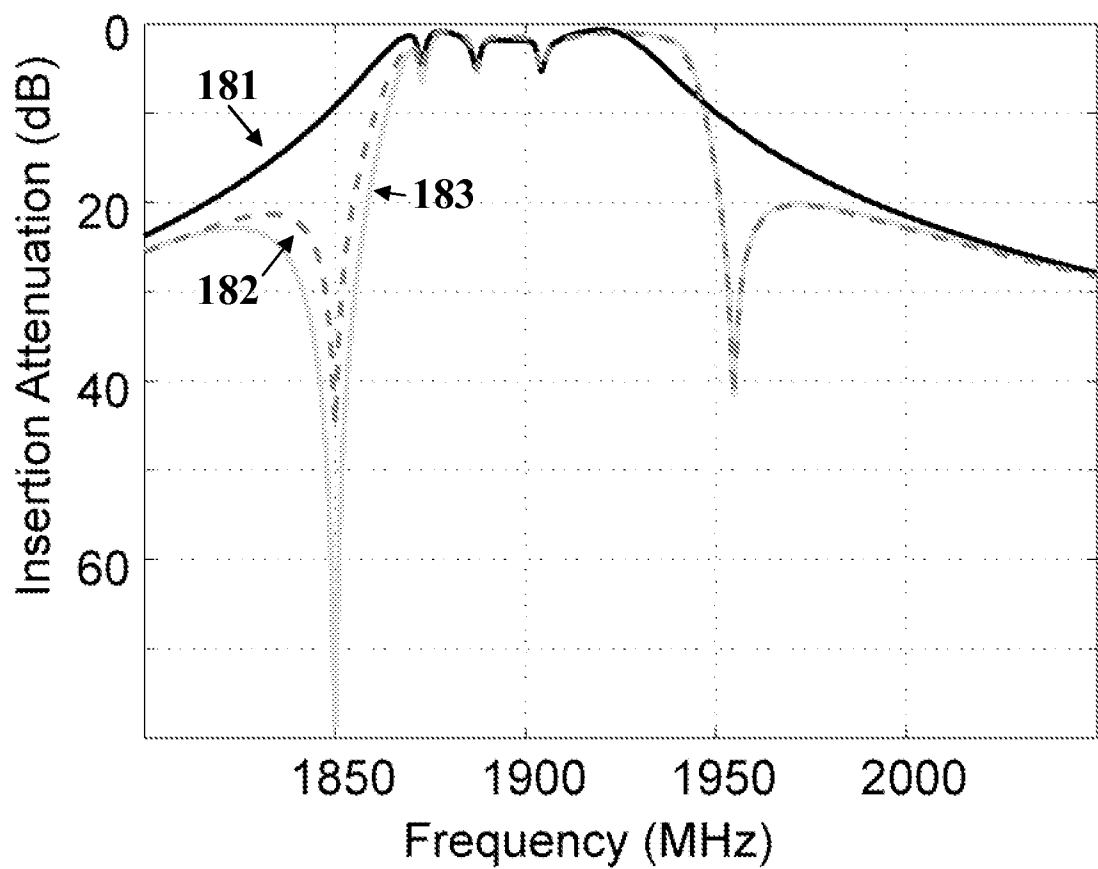


Fig. 20

**PATENTTI- JA REKISTERIHALLITUS**

Patentti- ja innovaatiolinja  
PL 1160  
00101 Helsinki

**TUTKIMUSRAPORTTI**

<b>PATENTTIHAKEMUS NRO</b>		<b>LUOKITUS</b>
20106063		Int.Cl. <b>H03H 9/56</b> (2006.01) <b>H03H 3/02</b> (2006.01)
<b>TUTKITUT PATENTTILUOKAT</b> (luokitusjärjestelmät ja luokkatiiedot)		ECLA H03H 9/56F H03H 3/02
IPC: H03H		
<b>TUTKIMUKSESSA KÄYTETYT TIETOKANNAT</b>		
EPO-Internal, WPI, XPI3E		

**VIITEJULKAIKUT**

<b>Kategoria*)</b>	<b>Julkaisun tunnistetiedot ja tiedot sen olennaisista kohdista</b>	<b>Koskee vaatimuksia</b>
X	MELTAUS et al. 'Laterally Coupled Solidly Mounted BAW Resonators at 1.9 GHz' Julkaisussa IEEE International Ultrasonics Symposium 2009. IEEE, 2009, s. 847-850. tivistelmä; luvut 1, 2, 3 ja 4; kuvat 1, 2, 3 ja 4; taulukko 1	1-14, 17
Y		15, 16
Y	WO 2006126168 A1 (KONINKL PHILIPS ELECTRONICS NV) 30. marraskuuta 2006 (30.11.2006) sivu 4, rivit 1-25; sivu 13, rivit 8-27; sivu 14, rivit 3-26; sivu 15, rivit 1-12 ja 30-32; sivu 16, rivit 1-10 ja 16-32; sivu 17, rivit 1-3 ja 21-31; sivu 18, rivit 1-8 ja 16-26; sivu 19, rivit 1-2; kuvat 1, 2, 5 ja 16-21	15, 16
A	ALLAH et al. 'Solidly Mounted Resonators with Layer-Transferred AlN using Sacrificial Crystalline Surfaces'. Julkaisussa Proceedings of the European Solid State Device Research Conference, 2009. ESSDERC 2009. IEEE, 2009, s. 375-378. luku 3 ja kuva 2	17

**Jatkuu seuraavalla sivulla**

\*) X Julkaisu, jonka perusteella keksintö ei ole uusi tai ei eroa olennaisesti ennestään tunnetusta tekniikasta.  
Y Julkaisu, jonka perusteella keksintö ei eroa olennaisesti ennestään tunnetusta tekniikasta, kun otetaan huomioon tämä ja yksi tai useampi samaan kategoriaan kuuluva julkaisu yhdessä.

A Yleistä tekniikan tasoa edustava julkaisu.

O Tullut julkiseksi esitelmän välityksellä, hyväksikäytämällä tai muutoin muun kuin kirjoituksen avulla.

P Julkastu ennen hakemuksen tekemispäivää mutta ei ennen aikaisinta etuoikeuspäivää.

T Julkastu hakemuksen tekemispäivän tai etuoikeuspäivän jälkeen ja valaisee keksinnön periaatetta tai teoreettista taustaa.

E Aikaisempi suomalainen tai Suomea koskeva patentti- tai hyödyllisyysmallihakemus, joka on tullut julkiseksi hakemuksen tekemispäivänä (etuoikeuspäivänä) tai sen jälkeen.

D Julkaisu, joka on mainittu hakemukseissa.

L Julkaisu, joka kyseenalaistaa etuoikeuden, osoittaa toisen julkaisun julkaisupäivämäärän tai johon viitataan jostakin muusta syystä.

&amp; Samaan patenttiperheeseen kuuluva julkaisu.

**Tämä asiakirja on koneellisesti allekirjoitettu.****Lisätietoja liitteessä****Päiväys**

11.08.2011

**Tutkijainsinööri**

Mika Kämäräinen

Puhelinnumero +358 9 6939 500